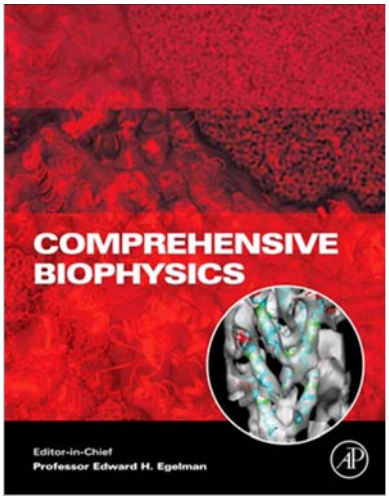

From D.N. Robinson, Y.-S. Kee, T. Luo and A. Surcel, Understanding How Dividing Cells Change Shape. In: Edward H. Egelman, editor: Comprehensive Biophysics, Vol 7, Cell Biophysics, Denis Wirtz. Oxford: Academic Press, 2012. pp. 48-72.
ISBN: 978-0-12-374920-8

7.5 Understanding How Dividing Cells Change Shape

DN Robinson, Y-S Kee, T Luo, and A Surcel, Johns Hopkins University, Baltimore, MD, USA

Abbreviations

AFM	atomic force microscopy
BLCBS	both light chain binding sites
BTF	bipolar thick filament
CM	contractile meshwork
CR	contractile ring
E	elastic modulus
ELC	essential light chain
ELCBS	essential light chain binding site
F	force
FRAP	fluorescence recovery after photobleaching
L_c	contour length
L_p	persistence length (depending on the context of usage)
L_p	length of cortex tether pulled into micropipette (depending on the context of usage)
LCBS	light chain binding site
LTM	laser-tracking microrheology
MPA	micropipette aspiration
MSD	mean square displacement
R	putative myosin II BTF receptor
R	radius
R_f	radius of the furrow
R_p	radius of the pipette
RLC	regulatory light chain
RLCBS	regulatory light chain binding site
T	tension

Glossary

Cleavage furrow The indentation at the center of a dividing cell, which ingresses into a bridge that connects the two daughter cells.

Compressive stress The net stress that acts against the outward flow of cytoplasm from the cleavage furrow. It comprises the Laplace-like pressure from the daughter cells, polar cortical contractions, and viscoelastic cytoplasm.

Contractile meshwork The contractile structure at the cleavage furrow of a dividing cell composed of a noncircumferentially arrayed network of actin polymers.

Contractile ring The contractile structure at the cleavage furrow of a dividing cell composed of antiparallel actin bundles organized in a circumferential ring.

Cortex The region of the cell underlying the plasma membrane that is rich in actin cytoskeleton, including myosin II.

Cortical tension The force in the cell cortex that serves to minimize the surface area to volume ratio.

Curvature A mathematical term that describes how the geometry of a surface deviates from being flat. The curvature κ of a sphere is $2/R$, where R is the radius of the sphere; κ of a flat surface is zero as it can be treated as a sphere with an infinite radius.

Cytokinesis The physical separation of a mother cell into two daughter cells.

 doi:10.1016/B978-0-12-374920-8.00705-0

Duty ratio The fraction of time a motor protein spends bound to its track relative to the duration of its entire ATPase cycle.
Elastic deformation The deformation in which the mechanical stress is linearly proportional to the resulting mechanical strain.
Elastic modulus The proportionality constant describing the amount of mechanical stress required to impose a certain amount of strain on a material during elastic deformation.
Equatorial cortex The central region of the cell cortex that generally gives rise to the cleavage furrow.
Global cortex The region of the cortex outside of the cleavage furrow. This is also referred to as the polar cortex.
Laplace pressure The pressure generated at a curved fluid surface due to surface tension. It serves to minimize the surface area to volume ratio.
Mechanical phase angle The relationship between the elastic and viscous components of a viscoelastic material.
Mechanical stress The pressure (force per unit area) applied to a material.
Mechanosensing The ability to sense and respond to mechanical inputs.
Mechanotransduction The conversion of a mechanical input into a biochemical signaling pathway.
Mitotic spindle The microtubule structure that separates the sister chromatids during mitosis. The mitotic spindle also transmits signals that initiate mechanical and biochemical changes in the equatorial and global cortices of a dividing cell.
Myosin II A motor protein that binds to and performs mechanical work on actin filaments. Myosin II forms the basis of cellular contractility.
Persistence length The persistence length (L_p) is a parameter used to describe semiflexible polymers. When polymer length is longer than L_p, the polymer is flexible. For polymer lengths shorter than L_p, the polymer behaves like a rigid rod.
Radial stress These are the active stresses, thought to be generated primarily by myosin II, that act at the cleavage furrow.
Sarcomere The repeating contractile unit, consisting of actin polymers and myosin II bipolar thick filaments, found in muscle.
Stretch modulus The proportionality constant describing the viscoelasticity in the plane tangential to the surface.
Viscoelasticity A property of a material held together by dynamic interactions. These dynamic interactions lead to time-dependent responses to imposed stresses, leading to both viscous and elastic characteristics.
Viscosity The resistive property of a fluid to flow in response to an external stress.

7.5.1 Introduction

Cell division is an amazing cellular process in which a mother cell divides into two daughter cells in as little as five minutes. Cytokinesis requires every cytoskeletal polymeric network to operate together to ensure that the nuclear and cytoplasmic contents are evenly segregated into the two hemispheres that give rise to the daughter cells. These cytoskeletal networks drive the remodeling of the cell cortex as the cell pinches into two. Cytokinesis is elegant and spectacular, and is critical for normal development and in disease.[1] Many important developmental processes are coupled to cytokinesis, including stem cell decisions. Cells can manipulate cytokinesis to create highly asymmetrical cell divisions, such as the meiotic divisions during mammalian oocyte maturation and in embryonic cells.[2–4] Cytokinesis can also be suppressed altogether to create specialized cells such as the highly polyploid megakaryocytes, which will spend the remainder of their lives producing platelets, or polyploid cells like those found in the liver.[5,6] Numerous disease-causing mutations disrupt functions of proteins whose primary roles are to orchestrate cell division.[7,8] A number of excellent reviews have been written on cytokinesis already (e.g., Refs 9 and 10). Here, the focus will be on the current view of the physical aspects of cell division. Known parameters will be defined, how the cell manipulates them genetically, and how they work together to promote cell division. While these views have largely evolved from studying *Dictyostelium*, data will be incorporated from other systems and it will be shown where similarities and differences may lie. The authors' global view is that, at least for cells with a plasma membrane (meaning no cell wall), the core principles will prove to be universal. Apparent differences will likely reflect either specific details of individual systems or identify where understanding between these systems is still lacking.

7.5.2 Physical Parameters

Cytokinesis is inherently a mechanical process in which the cell deforms until a thin bridge is formed and ultimately severed to produce two daughter cells. To quantitatively assess the mechanical features of cytokinesis, basic physical parameters that govern the deformation of the surface of the cell must be defined. Two of these are the bending modulus (or bending energy), which is the proportionality constant describing the resistance to bending deformation perpendicular to the cell surface, and the stretch modulus, which is the proportionality constant describing the viscoelasticity in the plane tangential to the cell surface. To determine whether the energy cost of bending (bending modulus, B) or stretching (stretch modulus, S_c) is likely to dominate a particular cellular deformation, one can determine a characteristic length scale (l) defined as $l=\sqrt{(B/S_c)}$. From the published values for a *Dictyostelium* cell, $l \approx 50–100$ nm,[11] which implies that for a cellular deformation over micrometer-scale lengths (e.g., the width of a cleavage furrow), it is reasonable to consider that the energy cost from stretch will dominate. Other physical parameters affecting cell deformation include the curvature of the cell surface and the cortical tension, which in combination

give rise to Laplace-like pressures, and the viscoelasticity of the cytoplasm.

7.5.2.1 Membrane Surface Area and Membrane Remodeling

Plasma membrane surface area must expand during cytokinesis. If cell division occurs by conserving the volume of the cell, then from beginning to end the total membrane surface area must increase 26%.[12] Endocytosis and exocytosis are two processes known to affect membrane surface area. As such, genetic mutants in these pathways often have cytokinesis defects. Furthermore, some differences in lipid composition (including phosphoinositides) have been documented for the furrow membrane as compared to the daughter cell membranes, suggesting that these lipid compositions may play a role in regulating the cytoskeletons in each of these areas.[13–15] Another role for membrane reshuffling would be for the membrane to continuously remodel, relieving stress to prevent membrane tearing. Membrane by itself has time-dependent mechanics and will rupture with forces comparable to those experienced during cytokinesis and over the minutes timescale.[16] Interestingly, membrane surface area increases during cell spreading as well as cytokinesis, presumably to lower the membrane tension during these processes.[17] Therefore, two general roles for membrane remodeling are possible. First, membrane remodeling may be a permissive process, necessary to increase membrane surface area to protect the membrane as the cell surface area increases. Alternatively, membrane remodeling might play a very active role in the constriction mechanism, such as by promoting or driving the inward growth of the cleavage furrow membrane. With either scenario, defects in the process would lead to an impairment of cytokinesis. It is not clear yet whether one of the two scenarios dominates or if both contribute to different degrees. Nevertheless, mechanical studies of cells treated with the drug latrunculin (which depolymerizes the majority of actin polymers) indicate that ~90% of the cortical mechanical properties are contributed by the actin network.[18,19] Therefore, the membrane contributes only a small fraction to these parameters (cortical viscoelasticity and tension).

7.5.2.2 Cortical Tension and Cell Surface Curvature

Two physical parameters used to characterize cell cortex mechanics are cortical tension and cortical viscoelasticity (**Figure 1**). Cortical tension should be a major parameter that determines the dynamics of cytokinesis contractility. Generically, this is the composite of mechanical stresses that act at the surface of the cell. This includes forces acting normal to the surface as well as in the plane of the surface. In the most general sense, this can be thought of as the energy cost for adding a unit of surface area (A). Thus, the effective cortical tension (T_{eff}) is a complex parameter composed of a persistent portion (γ_0) and the strained elastic portion (stretch modulus, S_c) so that:

$$T_{\text{eff}} = \gamma_0 + S_c \frac{(A - A_0)}{A_0}$$

This cortical tension parameter then defines the energy cost for adding a unit of surface area to the cell. The cortical tension and curvature (κ) of the surface of the cell define the Laplace pressure (P) of the cell, whereby

$$P = T_{\text{eff}}\kappa$$

κ equals $1/R$ for a cylinder and $2/R$ for a sphere, where R is the radius of the cylinder or sphere. As a result, the cortical tension

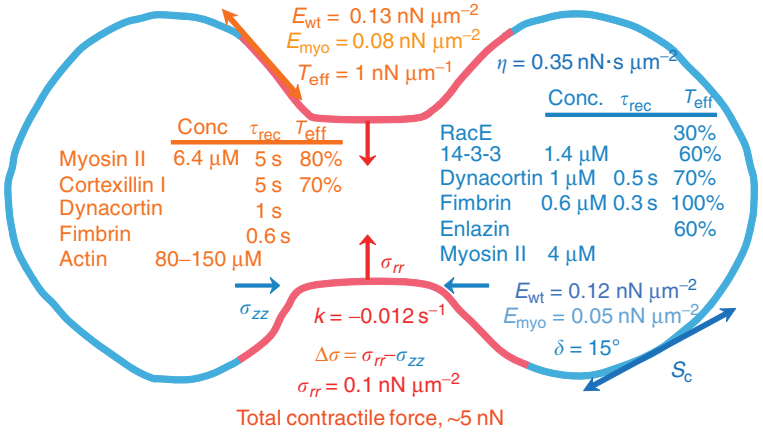

Figure 1 Cytokinesis by the numbers. The schematic presents an analytical framework for cytokinesis contractility and mechanics. The concentration of myosin II and various actin crosslinking proteins, their recovery time (τ_{rec}) from FRAP measurements, the reduction of the effective cortical tension (T_{eff}) of their mutants (based on single gene inhibition or deletion mutants) compared to that of wild type (1 nN µm^{-1}). The spatially resolved (furrow vs. global cortex) elastic moduli (E) for wild-type (E_{wt}) and *myoII* null (E_{myo}) cells are also provided along with the relevant wild-type cytoplasmic viscosity (η) and the cortical mechanical phasing (δ) based on particle tracking rheometry studies. The radial stresses (red vectors; σ_{rr}; with a magnitude of ~0.1 nN µm^{-2}) are antagonized by the compressive stresses (blue vectors; σ_{zz}), leading to a mechanical stress differential ($\Delta\sigma$). The radial stresses give rise to a total force of ~5 nN that drives furrow ingression. The stretch modulus (S_c) also describes the in-plane viscoelasticity of the cortex. Finally, the decay rate (k) for wild-type furrow ingression is also shown. Data summarized here are derived from several sources.[12,18,48,62,71,74,119]

initially acts to resist deformation of the mother cell, then later acts as an assistive element in the furrow region helping to squeeze cytoplasm from the bridge into the two daughter cells. The cortical tension of the daughter cells will continue to resist the flow of cytoplasm from the bridge region. Thus, one can see that the cortical tension will impact the furrow ingression dynamics in a complex manner by being resistive in two ways and assistive in another. First, the minimal force F that must act at the surface of the cell to initially deform it from a sphere is

$$F \propto T_{\text{eff}}/\kappa$$

Second, the positive push from cortical tension at the cytoplasmic bridge of radius R_{f} is given by

$$P = T_{\text{eff}}/R_{\text{f}}$$

Finally, the resistive stress from the Laplace pressure of the two daughter cells of radius R_{c} acting on the bridge is given by

$$P = 2T_{\text{eff}}/R_{\text{c}}$$

From its definition, it is known that the effective cortical tension is dependent on both persistent tension from osmotic pressure and perhaps motor proteins, as well as the material viscoelastic properties of the cytoskeletal network. Additional evidence for the relationship between osmotic pressure and the cortical actin-myosin II system has been provided for mitotic cell rounding, which precedes cytokinesis cell shape change.[20]

7.5.3 The Mechanical Parts List

The physical parameters that describe the macroscopic mechanics of cell division are dictated by the biochemical and mechanical properties of the molecular players. The list of proteins that contribute to cytokinesis is much larger than the few constituents mentioned here. Many of these are involved in signaling events that emanate from the mitotic spindle that ultimately control the mechanical changes of the cortex. Here, a bottom-up approach is taken, which is first to understand how the mechanics of cytokinesis works. Then, by defining and understanding these mechanics, it is possible to track back to the signaling pathways that regulate these mechanics. However, for the purpose of this review, the focus will be on the principal players that contribute directly to the mechanics and tying them into the signaling pathways where they are known to function.

For all animal cells, myosin II is considered the active force generator that drives the constriction of the cleavage furrow cortex[21–26] (**Figure 2**). Myosin II is a member of the myosin superfamily, which includes the unconventional and conventional myosins. While the superfamily of myosins traverse a broad array of cellular functions, including membrane anchoring (myosin I), actin polymerization (myosin I), vesicle trafficking (myosins V and VI), and contraction (myosin II), all members share a common motor domain that couples chemical energy from the hydrolysis of the γ-phosphate of ATP to conformational changes that allow the motor to perform

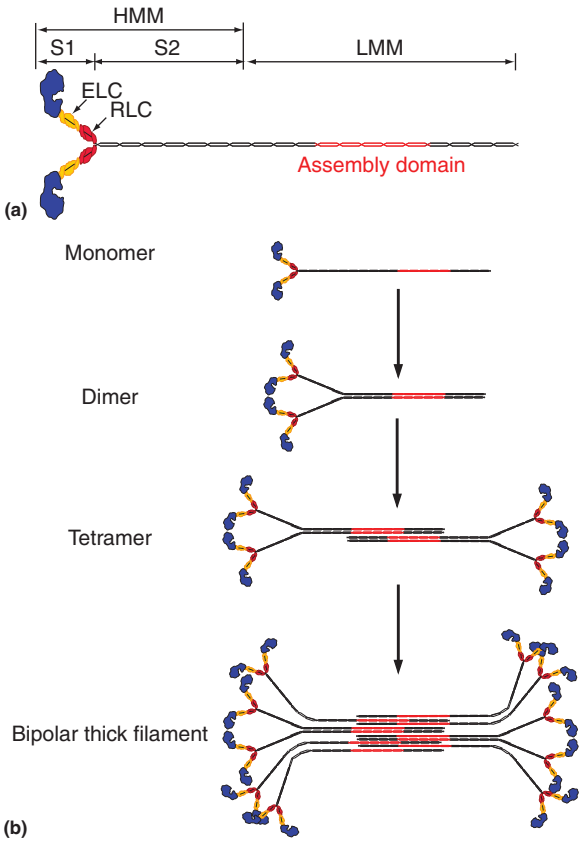

Figure 2 The anatomy of myosin II. (a) Basic domain structure of a single 'hexameric' myosin II monomer. S1 refers to the motor domain plus the lever arm, which binds the essential and regulatory light chains (ELC and RLC respectively). Heavy meromyosin (HMM) includes the S1 and the first part of the coiled coil region (the S2 region). HMM forms hexamers but cannot assemble into bipolar thick filaments (BTFs). The light meromyosin (LMM) region with the assembly domain mediates BTF assembly. (b) The assembly mechanism of a bipolar thick filament from assembly competent myosin monomers. From Figures 2.2 and 2.3 in Luo, T.; Robinson, D. N. The role of the actin cytoskeleton in mechanosensation. In: Kamkin, A.; Kiseleva, I., Eds.; *Mechanosensitivity in Cells and Tissues 4: Mechanosensitivity and Mechanotransduction*; Springer-Verlag: New York, **2011**; pp. 25–65. Copyright by Springer.

mechanical work.[27] The motile phase of the myosin ATPase cycle requires the myosin in the ADP · Pi state to bind first weakly, then strongly to an actin filament. The inorganic phosphate is rapidly released and the myosin undergoes its conformational change where it swings its lever arm through a $\sim 70^{\circ}$ arc, yielding a translocation of the myosin ~ 10 nm relative to the actin filament.[28,29] After this mechanical transition (the conformational change), the nucleotide binding pocket opens on the backside of the motor domain, allowing the ADP to release from the motor. At saturating cellular ATP levels, ATP rapidly rebinds so that the motor can release from the actin track.

This basic mechanochemical cycle is shared by all myosins but how each myosin responds to mechanical load (resistance) is a defining feature of individual myosin isoforms,

allowing them to tune to very specific tasks. In particular, the amount of force myosin can generate (and therefore the amount of tension required to stall the motor) is limited by the energy of ATP hydrolysis (~ 100 pN · nm). Therefore, in response to large mechanical loads, the motor has one of three choices: It can lock on to the filament (myosins I, II, and VI),[30–32] backstep (myosin V),[33] or release from the track altogether. These responses to mechanical load define the force–velocity relationships of how contractile systems will work. Furthermore, the load dependency is directionally dependent. For some of these motors, assistive pushes help the motor undergo its conformational changes and release from the track, while resistive pulls can slow or halt the motor. Processive myosin isoforms tap into this directionality to coordinate the two heads, ensuring processive walking along the actin filament.[34]

For myosin II, the soluble unit found in the cytoplasm is the hexameric 'monomer' (M), but the functional contractile unit is the myosin II bipolar thick filament (BTF) (**Figure 1**). The hexamers are formed from two heavy chains, where each heavy chain includes the motor domain, lever arm, and the coiled-coil tail.[29] The lever arm domain (a $\sim$9-nm-long α helix) consists primarily of two tandem light chain binding sites (LCBS), each approximately 30-amino-acid-long α helices. These LCBS domains are bound by light chains. The first light chain binding site closest to the motor (ELCBS) is bound by the essential light chain (ELC) and the second (RLCBS) is bound by the regulatory light chain (RLC). The RLC serves as the regulatory domain where in the unphosphorylated state the motor is in a less active configuration. This may be due to interactions either between the RLC and the motor (which inhibits the actin-activated ATPase activity) and/or the tail domain (which can inhibit bipolar thick filament assembly). Evidence exists for both types of interactions but may differ from isoform to isoform. RLC phosphorylation is believed to relieve these interactions, allowing the monomer to assemble into bipolar thick filaments and/or to prepare the motor for interactions with the actin polymer, which increases the actin-activated ATPase activity. For many nonmuscle myosins, the increase in V_{max} through light chain phosphorylation can be 20- to 30-fold, whereas in *Dictyostelium*, RLC phosphorylation increases the actin-activated ATPase activity just three- to fivefold.[35] The bipolar thick filament (BTF) size ranges from as few as eight to as many as 400 monomers in different organisms and tissue types.[36–40] Nonmuscle myosin II BTF assembly is also regulated by heavy chain phosphorylation. For *Dictyostelium* myosin II (PDB 1FMV), heavy chain phosphorylation converts the monomers into an assembly incompetent state driving them out of BTFs. Without phosphorylation, the myosin II assembles into BTFs characterized by a very slow release from the BTFs. Thus, total myosin II concentration is 3.4 μM with only $\sim$15–20% found in BTF form (i.e., 700 nM myosin II monomers in BTF form).[12,41] Similar observations have been made in metazoan cells.[42] Early evidence supported the notion that heavy chain phosphorylation stabilized a fold-back structure that prevents BTF assembly.[43] However, a careful structure–function analysis revealed that a tail fragment consisting of just the minimal BTF assembly domain followed by the regulatory domain (a region spanning 586 amino acids) recapitulates regulatable BTF assembly.[44] Overall, the heavy chain regulation results from subtle charge differences along the tail that promote or disrupt BTF assembly. It will be shown below that these properties of myosin II help specify the mechanical responsiveness of dividing cells and contribute to the mechanical stress generated in the cleavage furrow cortex.

The next major constituents of the cytokinesis shape change machinery are the actin polymers (PDB 3G37). These semiflexible polymers are assembled from globular actin and are highly dynamic with filament half-lives ranging from subseconds to several seconds. For a *Dictyostelium* cell, total actin is 250 μM and polymeric actin is $\sim$70 μM,[45–47] implying that most of the actin is sequestered in order to maintain an available pool of actin monomers. The actin polymers are distributed throughout the cortex and cytoplasm with a concentration ratio of cortical to cytoplasmic polymers of $\sim$1.2, making the cortical concentration $\sim$80 μM[48] (**Figure 3**). Using a DNase I inhibition assay, Podolski and Steck determined that the mean polymer length is 200 nm, though they observe that 70% of the polymers are less than 140 nm.[49] In

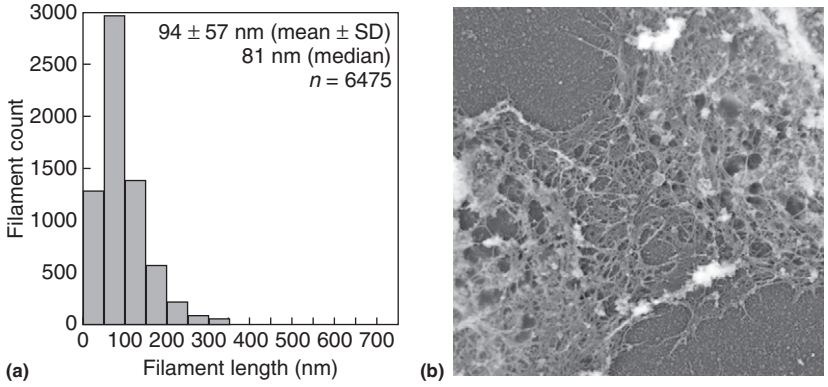

Figure 3 Actin polymers are distributed in a contractile meshwork in a number of systems. (a) The actin polymer length distribution for a *Dictyostelium* cleavage furrow cortex. (b) An image of a platinum-shadowed transmission electron micrograph reveals an actin meshwork in the cleavage furrow cortex. Figure derived from Reichl, E. M.; Ren, Y.; Morphew, M. K.; Delannoy, M.; Effler, J. C.; Girard, K. D.; Divi, S.; Iglesias, P. A.; Kuo, S. C.; Robinson, D. N. Interactions between myosin and actin crosslinkers control cytokinesis contractility dynamics and mechanics. *Curr. Biol.* **2008**, *18*, 471–480.

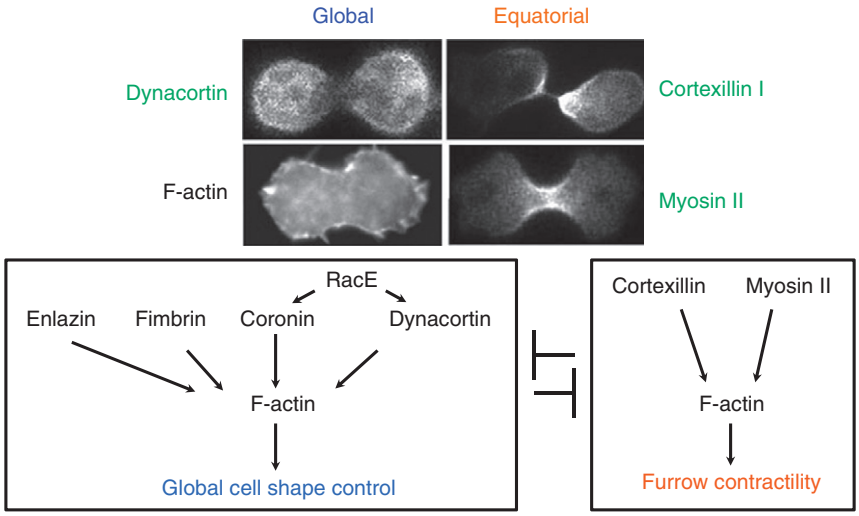

Figure 4 A two-module system of global and equatorial actin-associated proteins, including myosin II, controls the mechanics and dynamics of *Dictyostelium* cell division. From Octtaviani, E.; Effler, J. C.; Robinson, D. N. Enlazin, a natural fusion of two classes of canonical cytoskeletal proteins, contributes to cytokinesis dynamics. *Mol. Biol. Cell* **2006**, *17*, 5275–5286 and Robinson, D. N.; Spudich, J. A. Dynacortin, a genetic link between equatorial contractility and global shape control discovered by library complementation of a Dictyostelium discoideum cytokinesis mutant. *J. Cell Biol.* **2000**, *150*, 823–838. Copyright by American Society for Cell Biology, Rockefeller University Press.

spectacular agreement, the measured length distribution in the cleavage furrow was found to be 94 nm with a mean + 1 SD of 140 nm (~80% of the polymers should be less than the mean + 1 SD)[48] (**Figure 3(a)**). As is commonly observed in polymeric networks assembled with crosslinking and/or capping proteins, the length distribution is also somewhat skewed; assembled polymers without associated proteins tend to have exponential length distributions (e.g., Ref. 50). For comparison, the average actin polymer length in a *Schizosaccharomyces pombe* contractile ring is around 600 nm.[51]

The actin crosslinking proteins complete the contractile system (**Figure 4**). If the actin polymers are not tethered to each other or to the plasma membrane, the actin network would not contract, drawing the plasma membrane inward and constricting the cleavage furrow cortex. In metazoans, the major actin crosslinker is anillin, a multidomain protein that includes a pleckstrin homology (PH) domain, an actin binding domain and a myosin heavy chain binding domain.[52–54] In *S. pombe*, the distant but functional relative of anillin appears to be the Mid1 and Mid2 proteins, which share many of the same basic domain structures.[55–57] In *Dictyostelium*, the functional, but not structural, relatives are cortexillins I and II.[58] Cortexillins I and II may work as part of a functional unit with other co-factors.[59–61] However, the cortexillin I (PDB 1D7M) isoform appears to be the major player that works in cleavage furrow contractility and in the mechanosensory responses of the cell cortex (discussed below).[62–65] The cortexillin I domain structure includes an amino-terminal calponin homology domain followed by a coiled coil and completed with a small 93-amino-acid motif (cortICT) that includes two actin binding domains, the most carboxyl-terminal of which overlaps with a short PIP_2 (not PH domain-related) binding motif. Thus, cortexillin I can organize and anchor a complex actin network to the membrane. Cortexillin I, like myosin II, is most enriched in the equatorial cortex though significant populations are still found along the global/polar cortex.[12,18,63]

Other actin crosslinkers also play an important role in cell division. In *Dictyostelium* where this has been most closely examined, dynacortin, coronin, fimbrin, and enlazin make up the 'global' crosslinkers.[48,62,66,67] Average cellular concentrations for at least some of these crosslinkers (dynacortin and fimbrin) are of the order of 1 μM (**Figure 1**).[67,68] These crosslinkers are found most concentrated at the polar cortex though populations are found in the equatorial cortex. One can consider that myosin II/cortexillin I define one mechanical network (the equatorial network) and the global crosslinkers define the other mechanical network (the global network). These exist in inversely related gradients where the myosin II/cortexillin I network is most concentrated in the furrow cortex while the opposite holds true for the global network.[12,62,66] Significantly, these two modules of equatorial and global crosslinkers were originally discovered genetically.[62,66] A deletion mutant of *cortexillin I* was subjected to genetic suppression and the major suppressors were dominant-negative versions of dynacortin, enlazin, and coronin. Further, dynacortin overexpression induces a cytokinesis defect.[66] This phenotype was utilized to find similar proteins such as fimbrin that induced cytokinesis defects when overexpressed.[48] Finally, this global pathway is regulated by RacE, a Rac-family small GTPase.[66,69–72] *RacE* mutants have severe mechanical defects, and the actin crosslinkers dynacortin and coronin do not accumulate at the cortex in *RacE* null cells. Therefore, this small GTPase appears to control the global pathway of crosslinking proteins. As will be discussed later, several of these genetic modifiers also interact in unique ways with myosin II to alter the contractility and cortical mechanics (**Figures 1** and **4**). More recently, RacE was also found to be required for cortical localization of 14–3–3 (PDB 1A4O), which in turn modulates cytokinesis contractility and mechanics by regulating myosin II distribution and dynamics (**Figure 1**).[73,74]

In the mammalian system, some of the best studied actin crosslinkers are α-actinin (PDB 3LUE) and filamin (PDB

3HOP). During cytokinesis, α-actinin behaves in a manner that is highly analogous to the 'global' crosslinking system of dynacortin and fimbrin in *Dictyostelium* by providing a braking function to slow furrow ingression.[75,76] When α-actinin was overexpressed, furrow ingression slowed down and the cleavage furrow cortex actin polymers became more stable. In contrast, in α-actinin-depleted cells, less actin accumulated at the cleavage furrow cortex, the primary furrow ingressed at a faster rate, and ectopic furrows formed along the cortex. Filamin, another widely studied actin crosslinker that contributes to cell mechanics,[77] is reported to be inhibited by cyclinB-cdc2 phosphorylation during mammalian cell division, suggesting that filamin may be inactive during at least part of cell division.[78] Consistently, filamin does not appear to have a major role in *Dictyostelium* cell division.[79] These observations raise the possibility that some actin crosslinking proteins are inhibited during cell division to allow for a different group of actin crosslinkers to dominate the mechanics of the cell. This is an intriguing idea, particularly when considering what needs to occur during different phases of the cell cycle. Due to its flexible hinge domains, filamin is well tuned to strain-stiffening mechanics,[80,81] which may be very beneficial during motility and for withstanding shape disturbances encountered during interphase. However, if the job of the cell is to divide through internal stress generation, strain-stiffening mechanics may be counterproductive.

Finally, septins (PDB 2QAG) are GTPases that assemble into hetero-oligomeric filaments, which organize into a membrane-anchored lattice.[82] Present in the cleavage furrow and bud neck cytoskeletons in a number of species, septins appear to provide a rigid scaffolding role. However, that role does not appear to be ubiquitous. It may also be that some cells complete division and maintain an intercellular bridge for some time similar to the stable ring canals found in *Drosophila* ovarian nurse cells and spermatocytes.[83] Interestingly, depletion of septins in *Caenorhabditis elegans* embryos causes asymmetric furrow ingression to become symmetrical (i.e., the furrow ingresses evenly from both sides of the embryo).[84] Thus, septins in this system must play a role in how the mechanical stresses are propagated through the cortex. However, because it is not clear how septins impact the biophysics of cell division, they will not be further emphasized here.

A physical understanding of the mechanics and biochemistry of cell division hinges upon the concentrations of the components in the system (**Figure 1**). By knowing the protein and protein assembly concentrations and structures (e.g., the actin polymer length distributions), one can constrain the number of possibilities and mechanisms. Furthermore, the combination of concentrations and polymer lengths are significant determinants of what the mechanical features of the cytoskeletal network are. From concentrations, potential stoichiometries and bound fraction for particular binding interactions may be estimated given the measured affinity and concentrations for a pair of proteins. When coupled with advanced imaging techniques such as fluorescence recovery after photobleaching or total internal reflection fluorescence imaging, the binding kinetics may also be assessed. In the case of motor proteins such as myosin II where the maximum forces generated per motor head are well known, knowledge of the localized concentration can allow estimations of the myosin-generated active stresses in the cytoskeletal network. By combining this information with estimations of the mechanical stresses at play, one can begin to place limits on the shifts in myosin duty ratio, for example. These data can then be used to define boundary conditions for potential biochemical parameters, which for cytoskeletal systems can translate into a framework for the mechanics of the system. Ultimately, the goal is to be able to account for the dynamics and mechanics of cytokinesis from the basic physical and biochemical mechanisms, and protein concentrations along with the biochemical activities of the proteins provide an essential step for making this connection.

7.5.4 Mechanical Features of the Cortical Cytoskeletal Network

The canonical view of cell division is that the actin filaments of the cleavage furrow cortex are organized into antiparallel bundles (a 'contractile ring', CR) that contract in a muscle sarcomeric fashion.[23,51,85] The myosins are interdigitated in the CR so that they contract the network much like a muscle sarcomere contracts through the shortening of the individual contractile units. Recent evidence suggests that actin assembly through the actin nucleating protein formin, which nucleates straight actin polymers, has further promoted this idea.[86–89] Furthermore, it is clear that actin polymers are arrayed in circumferential bundles in such systems as the *S. pombe* and in some mammalian cells such as HeLa cells.[23,51,85] These structures provide the basis of the 'contractile ring' hypothesis. However, there are numerous examples of cell types that do not have such a well defined ring structure. In adherent *Dictyostelium*, the actin polymers are found in a 'contractile meshwork' (CM) that is most concentrated along the lateral edges of cleavage furrow cortex[48] (**Figure 3(b)**). Meshworks have also been observed in adherent dividing fibroblast cells and many types of dividing embryonic cells.[90] These observations together raise questions about the causal relationship between contractile network structure and cytokinesis contractility. Therefore, in the next sections, more general principles of actin cytoskeletal mechanics and how they apply to cell division contractility will be discussed.

The mechanical features of the cortical actin polymeric network are an essential determinant of how cell shape evolves over time. Actin is a semiflexible polymer where the mechanical properties of the polymer vary depending on its length (the contour length, L_c). The persistence length (L_p) of a semiflexible polymer can be thought of as the minimum length between two points on the polymer where the two points become independent of one another. For actin, the L_p is $\sim$10–17 μm.[91] For $L_c > L_p$, the network will stiffen with greater applied strain (strain stiffening) as the undulations in the flexible filaments are pulled out. However, in living cells where the polymer lengths are 10- to 100-fold shorter than L_p ($L_c \ll L_p$), the core mechanical properties are governed by the actin polymer concentration, the lifetimes of the actin polymers themselves, and the density and lifetimes of the polymer entanglements, which are stabilized by dynamic actin crosslinking proteins (see, e.g., Refs 18, 48, and 92–95).

From this perspective, it becomes immediately apparent why regulators of polymer dynamics and actin crosslinkers are so important for cytokinesis cell shape change. The regulators of actin polymer assembly (profilin (PDB 2PRF) and nucleators, including Arp2/3 (PDB 1K8K) and formins (PDB 1UX5)) and disassembly (intrinsic actin ATPase activity and cofilin (PDB 1COF)) may set a steady state of actin turnover dynamics. For contractility, the lifetimes of the entanglements (connection points between individual polymers) play a particularly important role. Actin crosslinking proteins stabilize the entanglements so that the actin network is interconnected, allowing mechanical stress to propagate through the network. These crosslinkers also help define the timescale over which the network can relax in response to deformations, either internally or externally induced. In particular, actin crosslinkers and actin polymer lifetimes help determine the network relaxation time and the timescale over which the network can flow. For example, the lifetimes of these entanglements must be longer than the myosin strongly bound state time (τ_s) in order for myosin II to generate tension in the network. Furthermore, the binding lifetimes of the actin crosslinkers may also be load sensitive, and the flexibility within the crosslinkers themselves may contribute to this load sensitivity.

These physical interactions on the cytoskeletal network are at the center of cell shape change. Regulatory pathways modify these parameters in order to regulate where net contractility occurs. Therefore, understanding these properties and how they are generated is critical for understanding cell shape change. Cytokinesis cell shape change occurs over ~300 s and results from cellular deformations that span ~200–300 μm^2 of surface area. However, this process is driven by molecules and conformational changes that range from a few nanometers (actin crosslinker length, myosin II step size) to 100-nm length scales (actin polymer length, myosin II bipolar thick filaments) and that occur from a few milliseconds (myosin II strongly bound state time, τ_s) to a few seconds (e.g., overall recovery time τ_{rec} of cortexillin I or myosin II measured by FRAP analysis). Therefore, to attain a complete view, methods must be used to measure mechanics across a broad range of timescales and length scales. No single method can readily do this, so a suite of methods must be used. For cell division, passive rheology, micropipette aspiration, and atomic force microscopy have been the most heavily employed.

7.5.5 Dissecting Mechanics Across Variable Timescales and Length Scales

Particle tracking includes several flavors of methods that range from single to multiple particle methods and that allow a broad range of timescale mechanics to be assessed.[18,19,48,96] For particle tracking in general, the particles can be inserted into the cell or allowed to adhere to the surface where they report on the cortex. Other modifications of this method include applying forces to the beads through the use of optical tweezers or magnetic fields (used in combination with magnetic particles).[97–101] In laser-tracking microrheology (LTM), a low-power laser is focused on a carboxylated polystyrene bead.[102–104] Fluctuations of the bead deflect the laser, and these deflections are monitored by a quadrant photodiode detector, which provides high temporal (submillisecond) and high spatial (nm) information of the bead position. The mean square displacements (MSDs) of the bead at each correlation time (τ) allow frequency spectral information of the MSDs to be acquired. The magnitude of the MSDs provides information about the mechanical resistance of the environment. The power law dependency (γ) of the MSDs as a function of τ (such that $MSD \propto \tau^{\gamma}$) provides information on the solid-like ($\gamma = 0$) or fluid-like ($\gamma = 1$) nature of the surrounding material. Furthermore, in the subdiffusive range ($\gamma < 1$), the data can be converted into viscoelastic moduli spectra using the diffusion-based generalized Stokes–Einstein relationship,[103] such that:

$$|G^*| = \frac{2K_B T}{6\pi r \langle MSD \rangle}$$

where K_B is Boltzmann's constant, T is temperature, and r is the radius of the bead. From the power law dependency, the mechanical phase angle (δ) is also recovered so that the elastic storage modulus ($G' = |G^*| \cos \delta$) and the viscous loss modulus ($G'' = |G^*| \sin \delta$) can be evaluated.

The particle-tracking approach works very well for assessing the viscoelastic moduli up to 100 ms (10 rad s^{-1}) timescales for *Dictyostelium* cells. For the cortex, δ is ~15°, indicating that on short timescales (<200 ms) the cortex is largely solid-like with a slight viscous character. On longer timescales, two classes of superdiffusive behaviors (where $\gamma > 1$) are detected: one that initiates at 200 ms and one at 2 s.[19] In *myoII* null cells, the 200-ms superdiffusive behavior is severely attenuated, which might lead one to conclude that myosin II drives this superdiffusive behavior. However, latrunculin treatment, which depolymerizes actin, fails to inhibit the superdiffusive behavior and, more importantly, removal of the actin crosslinker dynacortin from the cortex of the *myoII* null cells significantly restores the activity. This result demonstrates that myosin II and actin crosslinking proteins can be antagonistic and can work together to define the context (mechanical environment) in which other active processes in the cell occur. These observations suggest that single gene/protein inhibition might lead one to assign a direct role for a protein such as myosin II in a process when its role may really be indirect. This is analogous to a real-life experiment in which one pulls the plug on the traffic signals of a city, leading to an eventual traffic jam. One could conclude that the power source of the traffic lights really helps to power the automobiles when in reality it powers the traffic signals, facilitating the flow of the traffic through the city.

Micropipette aspiration (MPA) can also be used to measure cortex mechanics and offers the option of positioning the micropipette over different regions of the cortex to measure the heterogeneity across the cell (e.g., the furrow vs. polar cortices).[48] Numerous historically important studies in the cytokinesis field, particularly those of Hiramoto,[105,106] have utilized MPA. With MPA, elastic and viscous moduli and cortical tension can be measured. To measure elastic moduli, aspiration pressure jumps can be applied to the cell and the resulting deformation (length of the tether pulled into the pipette (L_p), which is generally normalized by the pipette

radius R_p) can be measured as a function of time. With pressures at or below a certain critical pressure (ΔP_{crit}, the pressure at which $L_p = R_p$), a stable deformation that maintains a constant length is formed. Above ΔP_{crit}, the aspirated tether can continuously flow into the micropipette for many types of cells. Different models are used to interpret the response of cells to these deformations. If one assumes that the cell is largely solid-like (solid body model), then the initial deformation after the pressure jump can be used to determine an elastic modulus according to:

$$E = \frac{3m}{2\pi\varphi}$$

where φ is a geometric factor (generally $\varphi = \sim 2.1$) and m is the slope of the ΔP vs. L_p/R_p plot (i.e., $m = \Delta\Delta P/\Delta(L_p/R_p)$).[107] From this plot, an equivalent cortical tension (T_{eff}) parameter can also be determined as

$$T_{eff} \approx 2.2\frac{ER_p}{1-(R_p/R_c)}$$

Alternatively, the entire time-dependent deformation curve can be fit to an appropriate mechanical equivalence circuit.[108] Here, the elastic constant as well as one or two viscous dampers can be determined. Finally, if one assumes that the cell has a viscoelastic shell containing a viscous core (cortical shell liquid core model), the effective cortical tension is measured by determining ΔP_{crit} and analyzing the shape, according to the Law of Laplace:[107,109]

$$\Delta P_{crit} = 2T_{eff}\left(\frac{1}{R_p} - \frac{1}{R_c}\right)$$

For *Dictyostelium*, on the longest timescale (100 ms) where a viscoelastic modulus is meaningful, the $|G^*|$ is 0.1 nN μm^{-2}, and from its power law dependency, $|G^*|$ may extrapolate to 0.07 nN μm^{-2} on the 1-s timescale. However, from the mechanical equivalence circuit, the elastic modulus was measured at 0.07 nN μm^{-2},[108] whereas the solid body model gives 0.095 nN μm^{-2}.[48] Similarly, the solid body and the cortical shell liquid core models each give cortical tension values of 1 nN μm^{-1}. Thus, while it is tempting to debate which model or method is superior, in fact, at least for *Dictyostelium* cells, it appears that all of the models do a reasonable job of capturing the relevant continuum parameters of the cell cortex[48] (**Figure 1**).

Atomic force microscopy (AFM) has also been used for cytokinesis mechanical studies.[110–112] Here, AFM is primarily used to measure force–volume curves. Hertz contact mechanics have been widely used to determine the physical properties of the surface deformed by an AFM cantilever.[113] Thus, fitting the measured force–volume curve to a Hertz model, the bending modulus can be measured. This measurement is highly sensitive to the contact area between the cantilever tip and the cell, as well as cell thickness. Because of the sensitivity to cell thickness, there is a risk that the measurements are influenced by the underlying hard substrate. The appeal of the approach is that it can be used to measure the bending modulus in a spatially resolved manner. However, a limitation is that it measures primarily the bending modulus, which can certainly report on cytoskeletal changes such as the recruitment of myosin II bipolar thick filaments, but as described in Section 7.5.2 is unlikely to be the most relevant parameter for accounting for the mechanics and dynamics of furrow ingression. Nevertheless, this approach has been used to measure mechanical changes during cytokinesis, which revealed that the bending modulus increased in the cleavage furrow to higher levels than the cortex over the emerging daughter cells.[110,111]

7.5.6 Mechanical Properties of Cytokinesis: Active vs. Passive

In order to understand how all of these protein players interact with each other to generate and control cytokinesis mechanics, it is imperative to define what is meant by active vs. passive processes. In this chapter, active implies that there is direct chemical energy input (e.g., ATP) in the system, whereas passive implies that the energy source is largely thermally driven. However, because cells are living, the system is of course active and the passive mechanisms are affected by active processes. Furthermore, even in the passive mechanisms, the cell actively expresses the proteins (e.g., actin crosslinkers) that define the elastic nature of the cytoskeleton, which then specifies how stresses are stored in and propagated through the actin network. Therefore, the major distinction between active and passive mechanisms in the context of cell division is whether (or how) the motor protein myosin II and active force generation from actin assembly are involved. To further illustrate the essential nuances implied here, an entirely active contractile mechanism might involve the directed assembly of a contractile network and the contraction of that network by myosin II-mediated sliding of the actin polymers (much like the contraction of a muscle sarcomere) coupled to progressive disassembly of the actin network. In contrast, a mechanism with greater passive character might have a surface stress (force/area) in the cortical actin network that squeezes cytoplasm from the midzone. These stresses give rise to fluid dynamical pressures (Laplace pressures) that when coupled with the viscoelasticity of the actin network allow the cell equator to invaginate.

7.5.6.1 Active Stress Generation

Active stress generation occurs principally through two major mechanisms: motor proteins and polymer assembly. Polymer assembly can generate stress because forces (f) are generated at the tip of the polymer as subunits are added.[88] This mechanism is directly dependent on the concentration of free monomer (c_A), the kinetics of binding (k_+) and release (k_-), and the unit length increase (δ) with each newly incorporated subunit, as described:

$$f = \frac{k_B T}{\delta}\ \ln\left(\frac{k_+ c_A}{k_-}\right)$$

During cytokinesis, new bulk actin polymerization occurs primarily at the poles in many systems, and the actin nucleating factor Arp2/3 as well as its activators are found at the

poles.[114,115] This suggests that new actin assembly at the poles may contribute to stresses that propagate throughout the elastic cytoskeletal network.

For motors, the mechanical stress (σ) is related to the force production per myosin II head (F), the myosin II duty ratio, and the number of heads in bipolar thick filament form (n) per unit of surface area (SA) of the cortex, so that:

$$\sigma = \frac{n \times \text{Duty ratio} \times F}{\text{SA}}$$

To assess the stresses at the cleavage furrow, a variety of approaches have been used, including the Cylinder-Thinning Model (see Section 7.5.12). However, in one simple model developed by Yoneda and Dan,[116] the minimum force required to stabilize the furrow may be estimated according to

$$F = 2T_{\text{eff}}R_{\text{f}} \cos\theta$$

where T_{eff} is the effective cortical tension, R_{f} is the furrow radius, and cos θ is a geometric parameter that accounts for the extent of furrow ingression. This relationship predicts the minimal force requirements to stabilize furrow ingression to be biphasic, which matches the amount of myosin II accumulated at the cleavage furrow cortex.[12,116] For a *Dictyostelium* cell, this relationship predicts an F_{max} of ~7 nN with the amounts of myosin II being nearly sufficient to account for this total force.[12] However, Carlsson pointed out that in a sarcomeric, circumferentially arrayed CR, the F_{max} should also be dependent on the length of the bipolar thick filament (d), the length of the actin polymer (L), and normalized to the circumference (C) of the ring.[117] In this case,

$$F_{\text{max}} = \frac{n(\text{Duty ratio})F(d+L)}{2C}$$

Using reasonable estimates of the parameters, this model predicts contractile forces ~20- to 30-fold lower than those estimated from the Yoneda and Dan relationship. Some of these numbers can now be reevaluated, particularly the duty ratio, which can be estimated to be five- to tenfold larger than for unloaded myosin II.[65] Furthermore, Carlsson noted that the effective polymer length L could be much larger than the actual polymer length through stable crosslinking proteins. Given that the average polymer length in the cleavage furrow of a *Dictyostelium* cell is ~100 nm, if this model were to work, L would need to be of the order of 10 μm, implying that 100 actin filaments would need to be linked into a continuous network. With a cortical polymeric actin concentration of ~80 μM, an actin polymer mean length of 100 nm, and 36 actin monomers per 100 nm, a cell with a ~5-μm radius furrow, a cortex thickness of ~0.3 μm, and a furrow length of ~3 μm would have ~40 000 total filaments in the furrow. This also corresponds to ~2-μM filaments. Given that there are several actin crosslinkers on the 1-μM concentration range, each actin polymer is likely to be bound by multiple crosslinkers, making it highly likely that there is a continuous network around the cleavage furrow cortex (**Figure 1**).

Another model describes the forces during contraction of an actin bundle from motors but also considers the actin polymer turnover kinetics.[118] Here, contractile stresses can be generated by myosin motors, but by accounting for the disassembly of the actin, the filament motor density remains constant, allowing a nearly linear decrease in furrow diameter. A further tenet is that contraction can also be achieved with end-tracking crosslinkers and actin treadmilling, possibly accounting for constriction of cleavage furrows in the absence of myosin II. Furthermore, long-lived actin crosslinkers increase the effective force by allowing forces to be transmitted through the network, whereas short-lived crosslinkers contribute an effective viscosity (friction) thereby slowing the constriction rate.

Because active stresses represent a significant component of the mechanical system of the dividing cell, it is essential to determine the magnitudes of these stresses and compare them to the concentrations and molecular biophysical properties of myosin II. However, to determine the magnitudes of the stresses actually at work can be tricky. To date, the authors have applied four conceptually distinct approaches to determine the magnitude of these active stresses. First, from the total amount of myosin II (~100 000 hexamers), force/head (3 pN), unloaded duty ratio (0.6%), and the surface area of the cleavage furrow (75 μm^2), the predicted myosin II-generated radial stresses are estimated to be ~0.05 nN μm^{-2} and a total force of ~4 nN.[12,71] Second, the total force was estimated to be ~7 nN using the Yoneda and Dan equation (above).[12] This converts to ~0.08 nN μm^{-2}. Third, the active radial stresses could be estimated from the dynamics of furrow ingression (described below in Section 7.5.12), which predicted active radial stress generation to be ~0.1 nN μm^{-2}.[71] However, with greater understanding of the mechanics of dividing wild-type and *myosin II* null cells,[48] this 0.1 nN μm^{-2} could be an approximately twofold underestimate, bringing the estimated stresses up to ~0.2 nN μm^{-2}. Fourth, it is known from mechanosensory studies[65,119] that cells can contract against 8–15 nN of total force and stresses from 0.4 to 0.6 nN μm^{-2} can induce myosin II localization. Thus, it is reasonable that *Dictyostelium* myosin II can undergo a fivefold shift in duty ratio in the context of cleavage furrow ingression if the cell's specific mechanical scenario requires it. In sum, active myosin II-generated stresses are of the order of 0.1 nN μm^{-2}, yielding a total active force of 5–10 nN (**Figure 1**). These force magnitudes are in remarkable agreement with the few tens of nanonewtons measured for the much larger echinoderm eggs by Rappaport in the 1960s.[120]

7.5.7 Mechanical Interplay Between Myosin II and Actin Crosslinkers

Myosin II and actin crosslinking proteins contribute to cell mechanics but in complex ways. Particularly for myosin II, nearly every scenario has been observed for how it impacts the mechanics of *in vitro* and *in vivo* cytoskeletal networks. *In vitro*, myosin II can fluidize, stiffen, or contract the actin networks, depending on whether ATP is saturating or whether a particular actin crosslinker has been added.[121–125] *In vivo*, the story is just as complex. Myosin II has been implicated in fluidizing the network, contributing to cortical tension, elasticity, and bending modulus, or even having no effect.[98,126–129] These seemingly disparate observations and roles have led to little

consensus on the role of myosin II. However, it is concluded that the specific impact that myosin II will have on the mechanics of a cellular process depends on two parameters: (1) the nature of the actin crosslinkers that are working with the motor and how they respond to mechanical forces, and (2) whether the actin network is under mechanical stress.

Myosin II and crosslinking proteins, such as cortexillin I, dynacortin, fimbrin, and enlazin, all contribute to the viscoelasticity and cortical tension to differing extents. Actin crosslinking proteins, such as α-actinin and filamin, have been heavily characterized for their effects on the viscoelasticity of pure actin networks.[81,130,131] Furthermore, it has been shown that their impact is dependent on the concentration and the ratio of crosslinker to actin (C:A). The translation of these studies to living cells, where there are many crosslinkers present as well as myosin II mechanoenzymes, is only just beginning to be approached.[77] Significant insight into how this may translate *in vivo* can be found in the *Dictyostelium* crosslinkers that promote cytokinesis.[18,48] Dynacortin presents an important starting point. Dynacortin is a dimeric, rod-shaped protein that can crosslink and bundle actin filaments *in vitro*.[18,67] The dynacortin dimer can be divided into amino-terminal (N173 domain) and carboxyl-terminal (C181 domain) halves, which were originally defined from a library suppression strategy. C181 and N173 both bind and crosslink actin and the apparent affinities of each domain for actin are known.[18] Furthermore, different types of activity assays to measure crosslinking and bundling reveal an apparent K_M (the Michaelis constant) for these processes. Most significantly, the impact of these proteins on cortical viscoelasticity (and cytokinesis phenotypes) was measured. First, the cellular concentrations of each domain were found to match the measured K_M values for crosslinking and bundling. The N173 domain has a high affinity for binding actin but a lower affinity for crosslinking, suggesting that the protein would not crosslink on very long timescales (an interpretation later supported by FRAP analysis of the full-length dynacortin). Consistently, N173 showed timescale-dependent effects on cortical viscoelasticity $|G^*|$ on the sub-100 ms time frame, whereas C181 elevated $|G^*|$ across all measured timescales. These two domains also had distinct effects on cytokinesis morphology and dynamics. Overall, these results indicated that with a lot of bookkeeping, the *in vivo* phenotypes, including impact on cortical elastic properties and cytokinesis phenotypes, may be directly accounted for by cellular concentrations and *in vitro* measured activities.[18]

The impact of each crosslinker differs in a wild-type vs. *myoII* mutant strain, suggesting that myosin II influences the actin network structures and/or kinetics of the crosslinkers and indicating that each crosslinker is unique in its force sensitivity and contribution to cell mechanics.[48] For example, depletion of *dynacortin* from a wild-type background reduces $|G^*|$ by ~40%, whereas removing it from *myoII* null background reduces $|G^*|$ by only 25%. A similar difference in the level of contribution to the cortical tension is also observed. Interestingly, dynacortin has a slower off-rate in a wild-type strain (450 ms τ_{rec}) than it has in a *myoII* mutant background (290 ms τ_{rec}), suggesting that dynacortin holds on longer to the actin when myosin II is there to pull on it. In contrast, fimbrin has no detectable effect on cortical tension (measured on the ~1-s timescale) whereas it contributes to 50% of $|G^*|$ (measured on timescales from 1 to 100 ms) in a wild-type background. However, in a *myoII* mutant background, removal of fimbrin leads to detectable changes in cortical tension. These timescale-dependent effects are most likely due to differences of the off-rate of fimbrin in the wild-type and *myoII* mutant backgrounds. From FRAP analysis, fimbrin's τ_{rec} is 260 ms in wild-type cells and increases to 680 ms in *myoII* null cells. Not only does fimbrin's τ_{rec} increase, but the immobile fraction also increases. Thus, one possible interaction between fimbrin and myosin II is for them to antagonize each other. Myosin II may pull fimbrin off the actin network, or fimbrin may settle into larger bundled networks if myosin II is not there to rearrange the filaments. *In vitro*, myosin II can pull filaments from fimbrin-crosslinked bundles, consistent with both possibilities.[68] Cortexillin I has another complex relationship with myosin II, as will be discussed in detail in Section 7.5.9. However, from FRAP studies, cortexillin I has a much longer τ_{rec} of 5 s (10- to 20-fold longer than dynacortin and fimbrin).

During cytokinesis, the cleavage furrow cortex stiffens slightly while the polar cortex becomes more deformable[48] (**Figure 1**). However, particularly for the polar cortex, the low-strain regime is not fully accessible by micropipette aspiration, leaving a window of deformability unknown. Myosin II contributes to the cortical elasticity of both the equatorial and polar cortices. More specifically, *myoII* null cells show about a threefold reduction in the elastic moduli (E) for both cortical domains compared to wild-type myosin II-rescued cells. Given that there is only a twofold concentration differential of myosin II between the cleavage furrow cortex and the polar cortex, it is expected that myosin II would impact both cortical domains. Due to the difficulty in making these measurements during cytokinesis, similar E values have not yet been determined for the crosslinking proteins. However, the E value of the polar cortex and the τ_{rec} of the global crosslinking proteins in the polar cortex are essentially at interphase levels. Yet in the wild-type cleavage furrow cortex, the E value increases slightly, the cortexillin I immobile fraction increases, and the τ_{rec} values of the global crosslinkers localized in the furrow region also increase, all of which indicate that the cleavage furrow cortex is essentially strain-stiffened as it undergoes mechanical stress. Consistently, the uncoupler mutant myosin II S456L, which has wild-type ATPase activity but a tenfold lower unloaded velocity due to a one-quarter productive working stroke and a threefold longer ADP-bound time, rescued the E value of the cleavage furrow cortex to wild-type levels but to a lesser extent the polar cortex E value.[48] This observation indicates that internal mechanical stress may rescue the S456L mutant myosin II. Overall, these observations are consistent with increased stresses at the cleavage furrow cortex, which leads to increased apparent stiffness in this region of the dividing cell.

7.5.8 Role of Cell Surface Interactions

Ever since the *myoII* null mutants were recovered, a role for cell traction forces generated against the substrate has been appreciated. In the *Dictyostelium myoII* null case, cells can

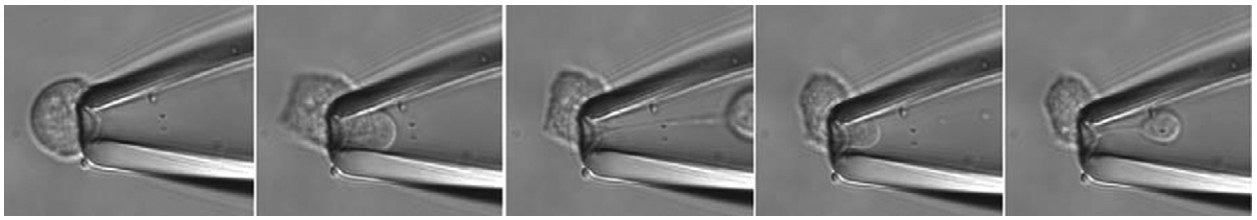

Figure 5 An illustration of a Laplace pressure in a living *Dictyostelium* cell. This *RacE* null cell was aspirated using a micropipette. The imposed mechanical stress elongates the cell and once the appropriate axial geometry is reached, a cytoplasmic droplet forms and pinches off.

complete mitotic cell division if adherent, whereas in the absence of adhesion they fail.[22,24,132] This led to the idea that these cells simply crawled apart, a process referred to as traction-mediated cytofission. However, the geometry of the dividing *myoII* null cells fails to support this. If the cells simply crawled apart, then volume conservation demands that for every tenfold decrease in diameter of the cleavage furrow cortex, the cells should move 10^2-fold apart (volume of a cylinder is proportional to radius r^2 and length l so that if r decreases tenfold, l must increase 100-fold). Therefore, as the cleavage furrow radius decreases from 10 to 0.1 μm (100-fold), the daughter cells should move apart 10^4-fold. In fact, the cells maximally increase their pole-to-pole distance by ~1.5-fold.[71] The answer is once again implicit in the Cylinder-Thinning Model (discussed below) and the viscoelastic nature of the cortex. Similar to a viscoelastic fluid where surface tension drives fluid neck thinning once the fluid lengthens to an axial (length to diameter) ratio of ~3:1,[133] the adherent *myoII* null cell elongates to an axial ratio of 2–3:1 and the Laplace pressure can drive the remainder of neck thinning. A demonstration using micropipette aspiration illustrates how surface stresses can drive neck thinning in cells so long as the appropriate axial ratio is achieved (**Figure 5**). Therefore, for mitotic cell division, *myoII* null cells only need to draw upon traction to generate the requisite shapes for cortical tension to take over and complete the furrow ingression process. In the absence of surface attachments, *myoII* null cells fail to elongate from the initial spherical mother cell.[132] In short, cells have one of two ways to escape from a round shape (phase 1 of cytokinesis): myosin II-mediated contractility or traction-mediated cell elongation. Once the cell enters phase 2, then passive Laplace pressure-mediated furrow thinning is sufficient.

These observations then beg the question as to how *myoII* null cells generate traction forces. In *Dictyostelium*, several genes that encode proteins involved in cell-substrate adhesion are involved. These include enlazin, which is the *Dictyostelium* ezrin-radixin-moesin family member, paxillin, talin family proteins (PDB 1MIX), and cell adhesion receptors.[62,134–137] Disruption or depletion of several of these genes leads to cytokinesis defects of variable severity. Enlazin is involved in cortical tension and cell-substrate adhesion, and contributes to *myoII* null cell division on substrates.[62] While full depletion or deletion of this protein appears to be lethal (or nearly so), partial knockdowns are viable, yielding cells that are 40% ($T_{\text{eff}} = 0.6$ nN μm^{-1}) softer than their parental control ($T_{\text{eff}} = 1$ nN μm^{-1}). These cells also make a smaller adhesive contact and adhere less tightly. Enlazin is enriched in the cortex and in cell surface adhesion sites. Significantly, when this protein is depleted from *myoII* null cells, these cells (*myoII*:enlhp) start division, contract much more slowly, and ~40% of the time stall during phase 2, ultimately regressing and failing at cell division. These observations suggest that as the *myoII* null cell elongates, the stresses must build up and be converted into tension so that Laplace pressure can drive cytoplasm from the equator. If the cell slips on the substrate, this conversion fails to occur. Double deletion of *myoII* and *paxillin* or *talin* similarly inhibits cell division, though the cells are less well characterized for how they are impaired.[135,137]

Analogously, a role for cell-substrate traction forces has been implicated in some types of mammalian cells, where dividing cells generate stresses against elastic substrates in the cleavage furrow region that are oriented perpendicular to the long axis of the cell.[138] Furthermore, mammalian cells can complete cytokinesis when myosin II is inhibited with blebbistatin so long as the cells are sufficiently adherent, demonstrating that similar principles are at work in these cells too.[139] It is noteworthy that nearly all of the studies so far discussed have been performed on two-dimensional substrates, whereas many cells divide in natural three-dimensional (3-D) contexts. Therefore, cells may need to sense these 3-D mechanical environments and to adjust their internal structures to compensate for asymmetries and perturbations imposed externally.

7.5.9 Mechanosensing and Mechanical Feedback

Originally, simple cells had to function in complex environments with changing temperature, salinity, nutrients, and mechanical inputs. Some of these physical inputs likely dictated the initial evolution of the signal transduction and mechanotransduction pathways that have been so well studied. In essence, the abilities of early cells to respond to these basic environmental inputs were usurped throughout evolution for higher-level functions, such as responding to chemoattractants by crawling cells, muscle contraction, hearing, and blood pressure regulation. Because cell division is such an important cellular process that must equitably separate the genetic and cytoplasmic contents into the two daughter cells, failure of the process leads to binucleated cells and/or asymmetries that can result in two daughter cells with considerably different volumes. Due to volumetric differences, cells may listen and respond to external cues in very different ways.[140] Sometimes these asymmetries are purposeful as in the meiotic cytokinesis events that produce the first and second polar bodies during mammalian oocyte maturation. Nevertheless, given that cytokinesis is mechanical and that cells divide in a variety of contexts, it was reasoned that mechanical feedback

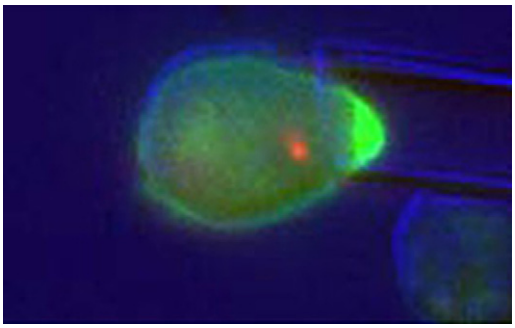

(a)

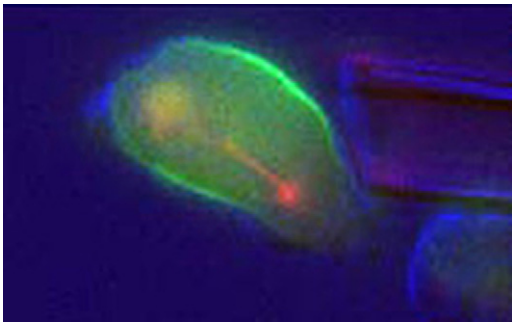

(b)

Figure 6 Cellular mechanosensing in a dividing *Dictyostelium* cells. (a) Cortexillin I accumulates in the cortex aspirated into a micropipette. (b) The cell then contracts away from the micropipette, allowing the cell to resume cytokinesis. Cortexillin I (green) is visualized by GFP, the mitotic spindle (red) is visualized with an mRFP-tubulin, and the micropipette is imaged by DIC (blue). Images reproduced from Effler, J. C.; Kee, Y.-S.; Berk, J. M.; Tran, M. N.; Iglesias, P. A.; Robinson, D. N. Mitosis-specific mechanosensing and contractile protein redistribution control cell shape. *Curr. Biol.* **2006**, *16*, 1962–1967.

would likely play a role in tuning the contractile apparatus and in shape control. Nonquantitative observations of dividing cells show a higher accumulation of myosin II at the cleavage furrow cortex when the cells were overlaid with a sheet of agarose to compress them. This further suggests that the ability of cells to sense surface stresses can affect myosin II enrichment at the cleavage furrow cortex.[141]

In search of such a feedback system, micropipette aspiration was used to apply stresses of the order of 0.1–1 nN μm^{-2} (similar to the magnitude of stresses that dividing cells are likely to generate at the cleavage furrow cortex) to the surface of cells[65,119,142] (**Figure 6**). This application of stress generates an outward deformation across a surface area of around 10–30 μm^2. For comparison, the surface area of the cleavage furrow cortex at the beginning of cell division is $\sim$200 μm^2, which reduces to 5–10 μm^2 near the end of division. The applied stresses induce myosin II and the actin crosslinking protein cortexillin I to accumulate at the micropipette in a mechanical stress magnitude-dependent manner. In this stress-induced redistribution of myosin II and cortexillin I, both the motor and crosslinker were interdependent, meaning if either protein was deleted the other protein failed to accumulate. None of the global crosslinking proteins (dynacortin, enlazin, or fimbrin) were required for the mechanosensitive localization, implying that cortexillin I plays a unique role. In particular, these observations suggested that myosin II and cortexillin I define a mechanosensory module. Given that myosin II is an active force generator, myosin II itself may be the active component of the sensor. Thus, cortexillin I would provide stable anchoring of the actin filaments, allowing the myosin II motor to generate force and thereby experience tension on the motor domain, locking it into the transition state. Finally, it was determined that altering the BTF assembly process negatively impacts the mechanosensory mechanism. Therefore, the authors found that this mechanosensory module has three critical elements: the myosin II active force generation dependent upon its mechanochemistry, myosin II bipolar thick filament assembly dynamics, and cortexillin I-mediated actin filament stabilization. Cooperativity between myosin II and cortexillin I then promotes their coordinated accumulation in response to mechanical stress.

To confirm the notion that myosin II is the active element of the sensor, the lever arm length was changed to determine if it would tune the pressure dependency of the mechanosensitive localization of myosin II.[65,143] It was found that a longer lever arm mutant generated by inserting an extra essential light chain binding site ($2 \times$ ELC mutant; 13-nm lever arm and 4 $\mu m\ s^{-1}$ unloaded actin sliding velocity) was more responsive than wild-type myosin II (9-nm lever arm and 3 $\mu m\ s^{-1}$ unloaded actin sliding velocity). In contrast, the deletion of both light chain binding sites (ΔBLCBS; 2-nm lever arm and 0.6 $\mu m\ s^{-1}$ unloaded actin sliding velocity) required much higher applied stress to undergo mechanosensitive localization and still failed to achieve wild-type response levels. The S456L mutant myosin, which has a wild-type lever arm and ATPase activity but a tenfold slower unloaded actin filament sliding velocity, showed almost wild-type mechanosensitive localization, ruling out the unloaded actin filament sliding velocity as the determinant. Finally, regulatory light chain phosphorylation was also required for mechanosensitive localization of the wild-type myosin. Importantly, all of the lever arm length mutants have full actin-activated ATPase activity, making the mutants behave like fully phosphorylated wild-type myosin II. This rules out arbitrary differences due to lack of myosin II regulation. Given that the F_{max} of the myosin motor is inversely related to lever arm length (assuming the lever arm is rigid),[143] these observations strongly suggest that myosin II mechanochemistry is an active element in the cellular scale mechanosensor. More specifically, this lever arm length dependency suggests that as the motor generates force, it experiences tension by pulling against an anchored actin filament. As a result of this tension, the myosin motor gets stalled in a force-sensitive mechanical transition state, causing the motor to remain tightly bound to the actin filament. For comparison, myosin II concentrated 1.5- to 2-fold at the micropipette tip, which is comparable to the level of concentration that occurs at the cleavage furrow cortex. Considering the applied stress and the number of myosin heads underlying the membrane at the micropipette, it was estimated that myosin II could undergo an approximately five- to tenfold shift in duty ratio. This is comparable to the

load-dependent shifts in duty ratio observed *in vitro* for other myosin II isoforms. These results are significant because it has often been proposed that such myosin-based mechanosensing operates in the highly disordered arrays of nonmuscle cells. However, because no direct proof had existed previously and given the number of proteins that are now known to display mechanosensitive behavior, it was possible that myosin II simply acted downstream as part of a mechanotransduction pathway rather than functioning as the upstream mechanosensor.

The second component of the mechanosensory module is the myosin bipolar thick filament assembly and disassembly dynamics. The bipolar thick filament assembly of many types of nonmuscle myosin II is regulated by heavy chain phosphorylation and dephosphorylation. Though the details of this regulation may vary somewhat from isoform to isoform, all mechanisms have a common output, which is to maintain a free pool of unassembled myosin monomers (hexamers) and dynamic bipolar thick filaments that can be constructed and disassembled rapidly in the cell in response to cues. For *Dictyostelium*, bipolar thick filament assembly is regulated by the phosphorylation of three critical threonines located downstream of the assembly domain. The phosphorylated myosin II leads to disassembly and prevents the assembly of the BTFs. Substitution of three aspartic acids ($3\times$Asp; a phosphomimic) for these threonines blocks BTF assembly and accumulation of myosin II at the cleavage furrow cortex and at the micropipette. In contrast, substitution of the threonines with alanines ($3\times$Ala myosin) mimics the unphosphorylated myosin II so that it constitutively assembles into thick filaments and turns over only very slowly by comparison to wild type. $3\times$Ala accumulates at the cleavage furrow cortex but fails to accumulate in response to mechanical stress. These observations indicate that myosin BTF dynamics are critical to rapid responses to applied mechanical stress through the mechanosensory pathway.

In the cell, ~80% of myosin II is found in the disassembled monomeric (hexameric monomer) state.[41] However, this unassembled pool of monomers is lost for the $3\times$Ala mutant myosin II or in cells where the myosin heavy chain kinases are deleted.[41,144] This implies that BTF assembly minimally requires assembly competent monomers with some unphosphorylated sites in the regulatory domain. Therefore, the first step of the BTF assembly pathway is the conversion of assembly incompetent monomers (M_0) to assembly competent monomers (M). *In vitro* studies[145,146] indicate that BTF assembly then occurs through a nucleation process in which two Ms form a parallel dimer (D), and two parallel dimers assemble into an antiparallel tetramer (T). A dimer is then thought to add on to the T, forming the first BTF (BTF_3), and dimers subsequently add on to BTF_n, forming BTF_{n+1}. Furthermore, the measured critical concentration for BTF assembly if all of the myosin is assembly competent is 20 nM, and addition of actin to the reaction eliminates the lag phase of assembly indicative of nucleation.[145,147] Finally, the largest BTFs are thought to consist of ~70 M per BTF.

Kinetic simulations using this model with measured kinetic or equilibrium constants for each of the steps based on *in vitro* experiments and *in vivo* FRAP analysis revealed interesting properties of the system[65] (**Scheme 1**). First, if a population of

$$M_0 \underset{k_{-1}}{\overset{k_1}{\rightleftharpoons}} M, \qquad k_1 = 0.0008\ s^{-1},\ k_{-1} = 0.1\ s^{-1}$$

$$M + M \underset{k_{-2}}{\overset{k_2}{\rightleftharpoons}} D, \qquad k_2 = 0.37\ \mu M^{-1}s^{-1},\ k_{-2} = 0.0\ s^{-1}$$

$$D + D \underset{k_{-3}}{\overset{k_3}{\rightleftharpoons}} T, \qquad k_3 = 0.0395\ \mu M^{-1}s^{-1},\ k_{-3} = 0.0045\ s^{-1}$$

$$T + D \underset{k_{-4}}{\overset{k_4}{\rightleftharpoons}} BTF_3, \qquad k_4 = 1.25\ \mu M^{-1}s^{-1},\ k_{-4} = 0.025\ s^{-1}$$

$$BTF_n + D \underset{k_{-5}}{\overset{k_5}{\rightleftharpoons}} BTF_{n+1}, \qquad k_5 = 10\ \mu M^{-1}s^{-1},\ k_{-5} = 0.2\ s^{-1}$$

Scheme 1 Assembly scheme for builing a myosin II bipolar thick filament. M_0 is the assembly incompetent monomer, M is the assembly competent monomer, D is the assembled dimer, T is the tetramer, and BTF_n is the bipolar thick filament with n dimers. The k values are the forward and reverse reaction rates. The completely assembled BTF is thought to consist of ~70 Ms.[145] The scheme is reproduced from Ren, Y.; Effler, J. C.; Norstrom, M.; Luo, T.; Firtel, R. A.; Iglesias, P. A.; Rock, R. S.; Robinson, D. N. Mechanosensing through cooperative interactions between myosin II and the actin crosslinker cortexillin I. *Curr. Biol.* **2009**, *19*, 1421–1428.

80% M_0 is maintained, then at steady state the BTF sizes are predicted to be distributed exponentially with the most frequent size being the minimal BTF, BTF_3. Second, the most sensitive step in the reaction scheme might be the conversion of M_0 to M. This leads to three possible mechanosensitive assembly mechanisms. In one possible mechanism, a phosphatase could be activated. A second mechanism is that the myosin heavy chain kinase (PDB 3LMI) could be locally inactivated. In both of these scenarios, the local ratio of M_0 to M would be shifted to allow for myosin BTF assembly. A third possible mechanism is that when motor domains in local mini-BTFs are stabilized in the transition state by mechanical stress, additional unassembled myosin M and/or M_0 may bind to the same actin polymer through cooperative interactions between motor domains along the actin filament. Once these motors are localized along a filament, the monomers may then directly incorporate into the BTF. *In vitro*, muscle and *Dictyostelium* heavy meromyosin II motor domains can bind with high cooperativity to the same actin filament when either the actin is complexed with Ca^{2+}, but not Mg^{2+}, or when the myosin-actin binding reaction occurs in the presence of low ATP, but not ADP.[148,149] A mutant myosin (G680V) that is kinetically trapped in the transition state also shows cooperative binding, whereas binding in the presence of ADP·vanadate, which traps the myosin in an earlier ADP·Pi state, shows no cooperativity. These observations, along with lever arm length dependency, provide a compelling mechanism whereby the myosin motors bind and are stabilized in the isometric transition state so that more monomers can bind cooperatively. This may allow for further BTF assembly. An additional component of this third possibility is that the increase in myosin BTF levels is due to direct incorporation of monomers into preexisting BTFs without the need to nucleate new BTFs. Of course, combinations of these three possible mechanisms are also feasible.

The third component of the mechanosensory module is actin filament stabilization by cortexillin I.[65] In order for the myosin motor domain to experience tension, the filament that the motor exerts force on must be anchored for timescales much longer than the motor domain remains bound. Single molecule studies to characterize cortexillin I-actin binding lifetimes were performed. In this assay, cortexillin I held on to actin with a dwell time of 550 ms over the force range of -2 to 2 pN, indicating that cortICT does not show load sensitivity over this low-force regime. Further studies examining larger forces may reveal some load dependency. However, 550 ms is already 200-fold longer than the myosin II unloaded strongly bound state time (2.4 ms) and may be 20-fold longer if the strongly bound state time increases tenfold in response to the mechanical stress. Therefore, even without additional load dependency, cortexillin I would appear to hold on to the actin filament long enough to provide an anchor against which myosin II can pull.

Because cortexillin I accumulates interdependently with myosin II, this indicates that cortexillin I is doing more than just anchoring the actin. For example, cortexillin I may bind actin cooperatively in a manner similar to myosin II.[148,149] Additionally, other studies have shown that cortexillin I and IQGAP proteins can associate by co-immunoprecipitation. The *Dictyostelium* IQGAP proteins do not have the calponin homology family actin binding domains found in higher metazoan IQGAP proteins.[59,150] IQGAP-cortexillin associations may put cortexillin I in a configuration that makes it available for mechanosensory responses. The cortICT domain not only has two identifiable actin binding domains, but also includes a carboxyl-terminal lysine-rich region that can bind to $PI(4,5)P_2$.[151] Therefore, cortexillin I could also anchor to $PI(4,5)P_2$ in the plasma membrane.

Yumura and colleagues suggested that the PTEN (PDB 1D5R) phosphatase, which accumulates at the cleavage furrow cortex like myosin II,[13] may accumulate at the micropipette ahead of myosin II.[152] This observation was interpreted to mean that PTEN may be further upstream than myosin II in the mechanosensory system. However, myosin II mechanosensitive concentration still occurs in the micropipette and in the cleavage furrow cortex in *PTEN* null mutants, whereas PTEN fails to accumulate beyond the levels initially seen in the membrane in *myoII* mutants.[152] These data in combination are consistent with the myosin II-cortexillin I system serving as the primary mechanosensor.

This mechanosensing system is more robust during cell division than during interphase.[119] Over pressure ranges from 0.1 to 0.6 nN μm^{-2}, most strains of interphase cells seldom show these types of mechanosensory responses to applied deformations, which are typically relatively small and do not produce membrane-cortex rupture. However, higher pressures can produce larger deformations and/or some membrane-cortex rupture, either of which may promote myosin II mechanosensitive accumulation in interphase cells.[129,152] Further, the authors have found that *RacE* null mutants, which behave in a very fluid-like manner, are highly responsive to applied mechanical stress and show myosin II and cortexillin I mechanosensitive localization during cell division and interphase.[65,71] Therefore, this mechanosensory system is active throughout the cell cycle but is masked during interphase, at least in part, by a RacE pathway. This masking may be overcome by larger deformations, membrane-cortex rupture, or perhaps other unknown pathways or genetic modifiers. This suggests that RacE activity may be effectively modulated (turned down) during cell division to allow cleavage furrow contractility and the myosin II-based mechanosensory system to be active. RacE cannot be completely turned off during cytokinesis since *RacE* mutants have strongly altered cleavage furrow ingression dynamics and RacE is essential for cell division in suspension culture. Qualitatively, global actin crosslinkers dynacortin and enlazin appear much more cytoplasmic during anaphase through telophase than they are during interphase. Since dynacortin distribution along the lateral cortex is RacE dependent, these observations indicate that the RacE pathway is dampened to promote the whole cell remodeling (cleavage furrow ingression), which leads to two daughter cells. Overall, these observations point out that the wild-type cortex changes its fundamental character during cell division in order to allow for cleavage furrow ingression.

7.5.10 Biochemical-Mechanical Feedback Loops

From the aforementioned studies, it is becoming apparent that cytokinesis occurs through the interfacing of biochemical and mechanical properties (**Figure 7**). Biochemistry, such as myosin II bipolar thick filament assembly and motor mechanochemistry, contributes to mechanical properties while mechanical stress changes myosin II and likely actin crosslinker binding lifetimes. Furthermore, mechanics are inherently linked to the morphology of the cell. Initially, cortical tension is a parameter that resists deformation, but later it assists cleavage furrow thinning. Finally, genetically distinct pathways control spatial mechanics. All of these properties naturally collide to make cytokinesis a control system that is governed by biochemical-mechanical feedback loops. The round mother cell can be thought of as a system that is in quasi-equilibrium, and the system must be pushed away from this stable position in order for cytokinesis to proceed. The signals from the mitotic spindle appear to be part of this initial destabilization.

In classic models, this instability can come from astral microtubules, which trigger the polar cortex to relax (so-called 'polar relaxation').[153] Analogously, the polar cortex becomes more deformable.[48] As the polar cortex becomes more deformable, regional tension begins to squeeze the cell, elongating it. This pathway appears to be controlled by the RacE small GTPase in *Dictyostelium*. RacE serves as an inhibitor of the furrow ingression, providing a braking function, as well as serving as an inhibitor of the mechanosensory pathway.[65,71] RacE also presides over a pathway of global crosslinking proteins: Actin crosslinkers dynacortin and coronin fail to accumulate in the cortex in *RacE* mutants.[66] Therefore, the microtubule network could antagonize this global Rac pathway, thereby promoting symmetry breaking in the round mother cell. A similar antagonism of Rac by the centralspindlin complex was recently proposed in *C. elegans*.[154]

Coordinately, central spindle microtubules or astral microtubules pointing towards the equator are thought to deliver cues to the equatorial cortex.[155–158] These cues are

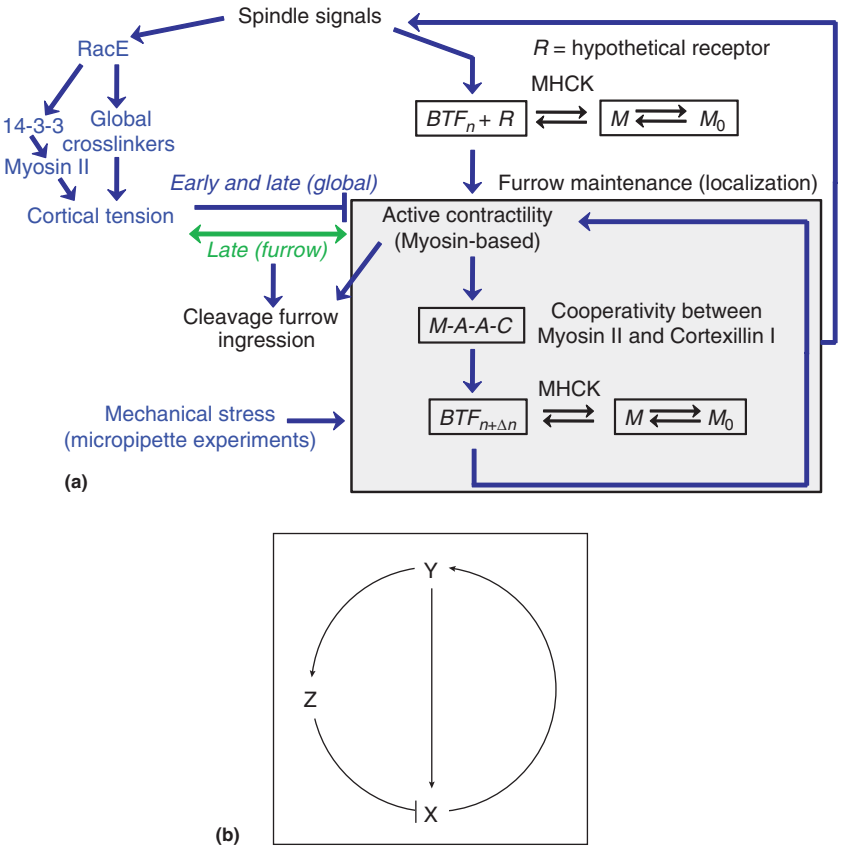

Figure 7 Cytokinesis occurs through integrated biochemical-mechanical feedback loops in *Dictyostelium*. Spindle signals modulate an equatorial pathway that leads to myosin II accumulation and equatorial contractility. A hypothetical receptor (R) or an active transport system might interact with an intermediate in BTF assembly to promote its localization in the cleavage furrow region. Micropipette studies reveal that mechanical stress can also direct myosin II and cortexillin I accumulation, which likely results in a positive feedback. This module likely also feeds back on to the spindle signaling proteins. The global cortex is modulated by a RacE small GTPase, which governs global actin crosslinking proteins, 14–3–3, and myosin II. This pathway controls global cortical viscoelasticity and cortical tension. This affects cytokinesis in two ways: first by inhibiting furrow ingression early during initial symmetry breaking, then cortical tension in the furrow cortex provides an assist to help drive furrow ingression. (b) This overall system has the basic structure of an incoherent negative feedback loop, similar to classic examples from control theory. From Surcel, A.; Kee, Y.-S.; Luo, T.; Robinson, D. N. Cytokinesis through biochemical-mechanical feedback loops. Semin. *Cell Dev. Biol.* **2010**, *21*, 866–873.

likely transported in part by microtubule-based motors such as the MKLP family members (kin6, MKLP1, kif12). These can then transport regulators of contractility such as Aurora kinase (PDB 2BFY) and INCENP (PDB 2BFY) in *Dictyostelium* and/or Rho pathway regulators such as MgcRacGAP (PDB 2OVJ) and ECT2 (not found in *Dictyostelium*, but implicated in *C. elegans*, *Drosophila* and mammalian cells).[159–161] These regulators might help direct the assembly of myosin II by activating Rho kinase (PDB 2F2U) (in metazoans), which promotes bipolar thick filament assembly. A yet to be discovered or defined myosin II bipolar thick filament receptor (R) and/or an active transport mechanism must also be implicated at this step because in *Dictyostelium*, as well as in mammalian cells, headless myosin II heavy chains (mutant forms of myosin heavy chain where the motor domain has been deleted) can still localize to the cleavage furrow of otherwise *myoII* null cells so long as the cleavage furrow begins to form.[162,163] Furthermore, in a variety of systems, myosin II can transiently associate with the furrow cortex in the presence of actin destabilizers such as latrunculin.[164] These observations imply that activation/formation of R may not be the most upstream event as its appearance only becomes revealed once the cell has elongated and a furrow begins to ingress. Furthermore, because BTFs are likely to be distributed in size, it is possible that R only needs to bind a small stable BTF nucleus, so that peripheral myosin monomers are free to associate/dissociate with the BTF nucleus.

From the mechanosensory studies, myosin II in cooperation with cortexillin I can redistribute in response to applied mechanical stress. Intrinsic mechanical stress should also be able to direct accumulation of these proteins. This mechanical stress-induced accumulation requires the full wild-type bipolar thick filament dynamics and possible cooperative binding of the myosin motor domain to actin. The mechanical stress-induced myosin II-cortexillin I accumulation also leads to local recruitment of a mitotic spindle signal factor. Thus, intrinsic mechanical stresses that propagate through the actin network from either cell elongation or from astral microtubules pushing

against the cortex may help activate myosin II-cortexillin I accumulation. Consistently, crosstalk between the microtubules and the contractile network through feedback has also been proposed for mammalian systems.[158]

Overall, cytokinesis is a large control system of integrated loops and feedback modules (**Figure 7(a)**) and has a basic structure of an incoherent negative feedback control system[165] (**Figure 7(b)**). This control system provides stability to the cell as it goes through its shape changes. The features of this control system might explain some discrepancies in the literature from other systems (described below in Section 7.5.14) and may also explain why certain features, such as the identity of the hypothetical myosin receptor R or myosin II targeting system, have been so elusive. However, with this view in hand, it may now be feasible to impair one or more of the feedback systems and design genetic screens that may assist in revealing these other mechanisms for myosin II accumulation as well as other important undiscovered cytokinesis proteins. In contrast, it may also mean that the machinery of the core cytokinesis mechanism is largely known and that the next goal is to see how it fits together to trigger symmetry breaking followed by furrow ingression.

7.5.11 Cleavage Furrow Ingression Through Three Mechanical Transitions

During cytokinesis, cells pass through a series of highly stereotypical shapes. In *Dictyostelium*, this shape evolution can be separated into three phases and three distinct mechanical transitions[11,12,71] (**Figure 8(a)**). The first phase (phase 1) encompasses the movement away from a spherical equilibrium position. In particular, the mother cell begins largely rounded with a 10-μm radius and elongates into a prolate ellipsoid (diameter of 8 μm and a length of ~12 μm). During this phase, myosin II begins to accumulate along the central 25% of the cell length (along the long axis of the cell). The peak myosin amount corresponds to the point at which the furrow begins to progress further inward. After this point, the furrow continues to ingress, marking the end of phase 1 and the beginning of phase 2 (the phase 1–2 transition). The myosin II concentration continues to increase, although the total amount of myosin at the cleavage furrow region is actually receding. Therefore, myosin II does not need to be further recruited to the cleavage furrow cortex; rather it may just need to be maintained. From FRAP studies, the myosin II continues to turn over with interphase dynamics (τ_{rec} ~5 s),[48,74,144] but it may be that there are core BTF nuclei that are maintained and peripheral monomers continue to exchange.[65] Phase 2 lasts until a thin bridge (~400 nm in diameter) is formed, which can dwell for some time before finally breaking. This final bridge dwelling phase defines phase 3. However, during phase 2, there is one additional mechanical transition that occurs right around the point at which the furrow length and furrow diameter are equivalent.[71] After this time, the furrow length crosses over to being longer than the diameter. This point is called the crossover length or D_x. For wild-type adherent *Dictyostelium* cells, the transition through D_x is smooth without a dramatic change in the furrow ingression dynamics. The process is nonlinear with a nearly exponential decaying diameter near the last part of the curve (**Figure 8(b)**). As soon as the mechanical features of the dividing cell are perturbed by any number of mutations (particularly myosin II, cortexillin I, dynacortin, RacE), then the furrow ingression dynamics change, in some cases dramatically, at the point of D_x. Particularly for *RacE* and *RacE/dynacortin* mutants, the cleavage furrow ingression dynamics can increase 30- to 50-fold faster than for wild type. The *myosin II* null cells also show a transition at D_x, though the increase in rate is not as dramatic as for the *RacE* mutants. Moreover, the furrow ingression dynamics, which reflect the time-dependent shape evolution, and the value of D_x are fingerprints of wild type and each mutant strain of cells. Thus, D_x is a highly significant parameter for the furrow ingression process and seems to strongly reflect features of the underlying mechanics.

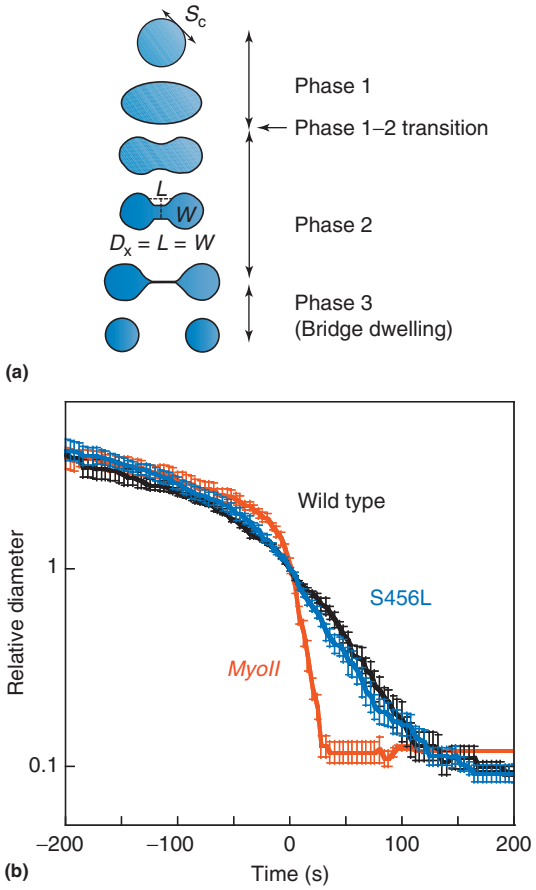

Figure 8 Cytokinesis contractility occurs through three phases with distinct kinetics. (a) A schematic diagram illustrates the stereotypical morphological shapes and the corresponding phases. Reproduced from Reichl, E. M.; Effler, J. C.; Robinson, D. N. The stress and strain of cytokinesis. *Trends Cell Biol.* **2005**, *15*, 200–206. The signature stage where the furrow length and width are equal, defining the D_x, is also shown. (b) The rescaled furrow ingression dynamics of wild-type, S456L, and *myoII* null cells are shown. The *myoII* null cleavage furrows undergo an abrupt transition near time 0 when D_x was reached. Reproduced from Reichl, E. M.; Ren, Y.; Morphew, M. K.; Delannoy, M.; Effler, J. C.; Girard, K. D.; Divi, S.; Iglesias, P. A.; Kuo, S. C.; Robinson, D. N. Interactions between myosin and actin crosslinkers control cytokinesis contractility dynamics and mechanics. *Curr. Biol.* **2008**, *18*, 471–480.

A recent study in *C. elegans* looking at the two-, four-, and eight-cell stage embryos indicated that furrow ingression occurred in a similar manner with an exponential tail.[166] This exponential crossed over to a linear decrease when the mitotic spindle structure was perturbed by silencing of a microtubule bundling protein. This observation may be equivalent to reducing the resistance of the network as observed in many of the *Dictyostelium* cytokinesis mutants and predicted for the Cylinder-Thinning Model (described below). Furthermore, the overall velocities of furrow ingression appeared to scale with cell size, so that the overall time to complete furrow ingression was relatively constant with changing cell size. The authors propose that this is due to a structural memory where the contractile ring is composed of a series of fixed-size contractile units that constrict with a constant velocity. Then, because larger cells have more contractile units, they constrict with a faster overall velocity. This idea is compatible with the concept that muscle contraction rate varies as the number of sarcomeres connected in series in the myofibril. However, in the absence of data about the viscoelastic properties of the equatorial and polar cortices and cytoplasm, the underlying mechanism remains to be determined.

7.5.12 Cylinder-Thinning Model

To account for the furrow ingression dynamics, a simple analytical model – the Cylinder-Thinning Model – has been developed that incorporates five simple parameters: cortical tension, radial stresses, compressive stresses, viscosity, and elasticity[71] (**Figure 1**). This model is readily applied to dividing cells with a relatively simple geometry where the furrow forms a clear bridge that interconnects the two daughter cells. Because of this geometry, the flow of cytoplasmic fluid from the furrow bridge to the daughter cells may be accounted for. This model considers that the push (outward flow) is driven by a Laplace-like pressure derived from cortical (surface) tension of the furrow region ($\Delta P_f = T_f/R_f$) and radial stresses (σ_{rr}) from myosin II (**Figures 1** and **5**). This push is resisted by compressive stresses (σ_{zz}) that act at the ends of the bridge. The compressive stresses are the net stresses that act against the outward flow and can arise from Laplace-like pressure from the daughter cell cortices ($\Delta P_c = T_c/R_c$), the polar/global cortical contractions, and the viscoelastic cytoplasm.

The cytoskeletal viscosity (μ) acts to dampen the flow of cytoplasm. This viscosity is nonlinear, being dependent on the relevant timescale, length scale, and applied force to the cytoskeletal material. Based on dimensional analysis, the velocity (v) of bridge recoil is likely to be governed by the ratio of tension (T_f) to the viscosity, so that

$$v = T_f/3\mu$$

For wild-type *Dictyostelium* cells, an effective viscosity of $\sim 0.35\ \mathrm{nN \cdot s\ \mu m^{-2}}$ is calculated from the measured cortical tension of $1\ \mathrm{nN\ \mu m^{-1}}$ and the recoil velocity of $1\ \mu\mathrm{m}^{-1}$.[71] This compares well with the largest, force-dependent viscosity of $0.35\ \mathrm{nN \cdot s\ \mu m^{-2}}$ measured for these cells using magnetic rheometry.[98]

To account for the furrow-thinning dynamics, two classes of models were considered.[71] The first class considered that the diameter of the bridge at time t ($a(t)$) is controlled by axial compression, where the Laplace pressure differential and radial stresses from myosin II are counterbalanced by the compressive stresses at the ends of the bridge and the viscosity. This model has the following form:

$$a(t) = a_0 e^{-\left(\frac{\Delta\sigma t}{6\mu}\right)} - \frac{T_f}{\Delta\sigma}\left(1 - e^{-(\Delta\sigma t/6\mu)}\right)$$

where a_0 is the initial diameter and $\Delta\sigma$ is the stress differential ($\Delta\sigma = \sigma_{rr} - \sigma_{zz}$). An implication from this relationship is that the furrow ingression dynamics will be more exponential initially but become more linear later. Second, the stress differential ($\Delta\sigma$) serves as a correction to the linear thinning.

The furrow ingression dynamics for wild-type, *myoII* null, and *RacE/dynacortin* mutant cells could be explained by using this analytical model.[71] In particular, the *RacE/dynacortin* mutant cells could be accounted for by essentially allowing the resistive stresses (σ_{zz}) to approach 0. In this case, a very rapid linear decrease is observed and velocities of furrow ingression approached $1\ \mu\mathrm{m\ s^{-1}}$ as predicted from the dimensional analysis (where $v = T_f/3\mu$). The *myoII* null furrow-thinning trajectory was accounted for by letting the radial stresses (σ_{rr}) approach 0. In this case, there is a very slow initial phase, but this crosses over to a faster linear decrease around the D_x time point, indicating that the geometry and cortical tension now dominate (**Figure 8(b)**). Finally, wild-type cells required that the cortical tension become counterbalanced by the resistive stresses so that the active myosin II-generated radial stresses could now drive the ingression mechanism.

Using this simple model, the furrow ingression dynamics and measured cortical tension values, the resistive stresses may be assessed. From the rate ($k \sim -0.012\ \mathrm{s^{-1}}$ and $k = -\Delta\sigma/6\mu$) of furrow decay in wild-type cells, the wild-type stress differential was calculated to be $0.025\ \mathrm{nN\ \mu m^{-2}}$. Based on the interphase mechanics of *myoII* null cells and an assumption that σ_{rr} is 0 (the assumption that myosin II is the primary source of σ_{rr}), σ_{zz} was estimated to be around $0.08\ \mathrm{nN\ \mu m^{-2}}$. By combining the $\Delta\sigma$ from wild-type and the σ_{zz} values from *myoII* null cells, wild-type σ_{rr} was inferred to be $\sim 0.1\ \mathrm{nN\ \mu m^{-2}}$. This is in good agreement with the stresses estimated from the myosin II concentrations ($0.05\ \mathrm{nN\ \mu m^{-2}}$) and the applied stresses that direct myosin II accumulation during mechanosensing ($\sim 0.4\ \mathrm{nN\ \mu m^{-2}}$). Overall, consensus appears to be emerging from the micropipette and furrow-thinning dynamics studies about the magnitude of the myosin II-generated active radial stresses at the cleavage furrow cortex, which is $\sim 0.1\ \mathrm{nN\ \mu m^{-2}}$.

The wild-type case is more complicated because the model requires that the effects from Laplace pressure are nearly eliminated. One way this could easily occur is if the myosin II strain-stiffens the network so that elastic effects dominate. In this case, time-dependent thinning would be determined in large part by elastic relaxation. This effect is also accounted for by the Cylinder-Thinning Model and can be described as the following, where G is the elastic modulus:

$$a(t) = \left(\frac{a_0}{T_c} G e^{-t/\tau}\right)^{1/3}$$

This expression predicts an exponential decay of furrow ingression with a characteristic time constant of ~80s. This 80-s time constant is approximately two orders of magnitude longer than the elastic relaxation times measured in interphase cells using magnetic rheometry. However, it is entirely possible that a different elastic time constant is relevant over the length scale and timescales of a cleavage furrow cortex. Therefore, it is likely that elastic relaxation also contributes along with compressive stresses to wild-type furrow ingression. The authors favor compressive stresses as the major determinant since they predict the nonlinear decreases observed for many of the mutants.

Though this model places a primary role for the mechanics of the cytoskeletal network, the notion that fluid pressures contribute to the flow of cytoplasm is implicit. Furthermore, pressure from a much lower viscous, noncompressible cytoplasm readily contributes to the tension in the cortical cytoskeleton. Thus, new ideas such as poroelasticity are compatible with the Cylinder-Thinning Model.[167,168] Poroelasticity largely implicates a biphasic cellular medium in which an interconnected elastic cytoskeleton is filled with a viscous cytoplasm. Indeed, from the diffusion coefficient (~30 $\mu m^2\,s^{-1}$) measured for the small GFP protein, the cytoplasmic viscosity experienced by a particle this size is only about threefold more than for water (10^{-6} nN · s μm^{-2}).[169,170] Therefore, the surrounding cytoplasm has a 10^4- to 10^5-fold lower viscosity but can contribute to the osmotic pressure, which in turn would contribute to the cortical tension and fluid pressure (ΔP) of the cell. Indeed, direct visualization of the water phase of the cytoplasm has been achieved by coherent anti-Stokes Raman scattering microscopy.[171]

A different model for cytokinesis contraction also emphasizes viscous dissipation as a determinant in furrow ingression kinetics.[172] This particular model invokes an increase in actin concentration to account for the reduced rate of late-stage furrow ingression. In *Dictyostelium* and many other systems, the actin concentration remains constant.[48] It is formally possible that accumulation of myosin II thick filaments, which concentrate about twofold during the constriction process, could explain the nonlinear dynamics. Consistent with this, cells expressing the 3 × Ala myosin II (a mutant myosin II that is deficient in heavy chain phosphorylation regulation of BTF assembly), which overaccumulates about threefold compared to wild-type myosin II, require more time to complete cleavage furrow thinning.[12] However, mutants such as *cortexillin I* and *RacE* accumulate wild-type myosin II at the furrow, suggesting that the concentration of myosin II bipolar thick filaments in and of themselves is not the explanation for the nonlinear dynamics observed for wild-type cell division.

7.5.13 Contractile Rings: The *Schizosaccharomyces pombe* Case

Schizosaccharomyces pombe cells assemble a well structured circumferential array of actin polymers. Though reports of the total cellular concentrations of actin vary widely, the assembled ring by all accounts is composed of ~500–1500 dynamic actin filaments (20 filaments per cross section) that are ~0.6–1 μm in length and oriented in an antiparallel fashion.[51,173–175] These filaments are believed to be assembled from several tens of membrane-bound nodes of the anillin-related protein Mid1p, which recruits several other proteins through sequential addition.[176,177] After Mid1p, the first of two myosin II isoforms followed by several other actin-associated proteins, including an IQGAP (a scaffolding protein), cdc12 (a formin), tropomyosin, α-actinin, capping protein, a second myosin II isoform, and septin, accumulate along the midzone. With the exception of actin, nearly all of the rest are found in submicromolar concentrations across the cell (e.g., overall concentration of myosin II is 0.45 μM, that of α-actinin is 0.22 μM, and that of Mid1p is 0.09 μM).[175] Upon assembly in the contractile ring, their concentrations can rise to micromolar range, with actin itself reaching nearly 0.5 mM. Most notably, there are ~2900 myosin II heavy chains (20 μM), corresponding to one bipolar thick filament (~14 heavy chains per BTF) per micron of actin filament (11-μm circumference · 20 filaments per cross section = ~210-μm linear actin). Interestingly, the myosin chaperone Rng3p is thought to be substoichiometric (though the ratios vary in different reports) with myosin II in the contractile ring.[175,178] However, at sufficiently high concentrations of myosin II (1 μM, which is well below the 20 μM found in the contractile ring), the *in vitro* unloaded actin sliding velocity reached full velocity without Rng3p.[178,179] Thus, Rng3p may contribute to a more subtle feature of myosin function, such as helping fold the myosin or providing stability when the myosin is put under load, rather than basic activation of myosin II motility.

Experimental evidence coupled with computer simulation has suggested that the *S. pombe* CR is built by the coalescence of the mid1p nodes, through a search–capture–pull–release mechanism.[180] In this model, cdc12 formin proteins catalyze new actin polymers, which extend from the nodes with the minus end pointing away from the nodes. Myosin II proteins at neighboring nodes grab these actin filaments, pulling them together to form a ring. Initially, upon formation, the nodes move diffusively ($D \approx 20\ nm^2\,s^{-1}$). Once cdc12 joins the node, actin filaments elongate, radiating in all directions from the node at a velocity of ~0.2 $\mu m\,s^{-1}$, and the nodes move directionally in 20-s bursts. Because at least some of the filaments appeared to span the full 4-μm width of the cell, this implies an actin filament lifetime of up to 20 s. However, this is likely an upper limit since other filaments were observed to disappear much more rapidly. Some filaments appeared to recoil, implying they were under tension, presumably from myosin II. These observations then allowed Monte Carlo simulations of the search–capture–pull–release model in which the major parameters include a myosin II radius of capture (100 nm), a force (4–6 pN) acting on the nodes (estimated from the velocity of the nodes and the apparent frictional coefficient of 0.2 pN · nm s^{-1} derived from the diffusion coefficient of the nodes), the actin polymerization velocity (0.2 $\mu m\,s^{-1}$; v_{pol}) and lifetime (20 s), the myosin II-actin association lifetime (20 s; τ_{break}), and a short-range repulsive force (10 pN) and radius of exclusion (150 nm) to prevent the nodes from overlapping. This basic model could recapitulate many aspects of the contractile ring assembly dynamics.

It is worth noting that nodes and mid1p are thought to be central to this search–capture–pull–release mechanism. However, myosin II rings can assemble in late mitotic, but not early mitotic, *S. pombe* cells in which Mid1p has been deleted and nodes therefore fail to form (e.g., Ref. 181). Activation of the septation initiation network, which activates constriction of the CR, was required for ring assembly in the absence of mid1p and cortical nodes. Further, electron microscopy reconstructions have been interpreted to imply that actin filaments assemble from a single spot and extend circumferentially, forming a belt.[51] One possibility is that fully active CR contraction can lead to organization of the ring, but if full contractility is not yet activated, then the search–capture–pull–release mechanism is needed to promote efficient ring assembly. The correlation between mitotic stage, nodes, and efficiency of CR assembly is further strengthened by the observations that cell cycle progression regulators are localized to the nodes.[182–184] These regulators are then negatively regulated by the dual specificity kinase pom1p, which is concentrated at the poles. As the cell lengthens, equatorial pom1p concentrations are depleted, allowing CR assembly. Thus, it may be a matter of regulation that nodes promote efficient CR assembly. Myosin II's involvement in node-mediated (search–capture–pull–release) and node-independent (contractility-dependent) assembly may reflect an intrinsic role of internal stresses, orienting the actin polymers into rings. Indeed, active myosin II is proposed to be required for both modes of ring assembly.[185] This common theme may imply that ring formation is a consequence of the context of contractility with mobile actin anchor points, rather than an essential intermediate necessary for contractility.

Contrasting the *S. pombe* system with the *Dictyostelium* system begs the following question: Why do *Dictyostelium* cells form CMs while *S. pombe* cells form CRs? All of the parameters used in the search–capture–pull–release model are known for *Dictyostelium*. From this, a few parameters emerge as being very different. Specifically, the actin filament number in *Dictyostelium* is 1–2 orders of magnitude higher, the polymer length is four- to tenfold shorter, τ_{break} is estimated to much shorter, and the v_{pol} is about tenfold faster (for at least rapidly assembling actin polymers though two populations of actin, the fast pool and a more stable pool exist in *Dictyostelium* cells).[186] Therefore, the tuning of these parameters may be sufficient to lead to a CM vs. CR. It would be interesting to see if these parameters may be tuned sufficiently to shift structures in one or the other of these systems. Alternatively, the geometry of an *S. pombe* cell is prolate ellipsoid, which has a radial symmetry about the cell. An adherent *Dictyostelium* cell has an inherent dorsal to ventral (top to bottom) polarity that may impose some asymmetry that promotes CM assembly.

7.5.14 Comparisons Between Systems

Historically, researchers of cytokinesis have touted the differences between the division systems found in different organisms. However, the authors would argue that the core physical principles are in fact common and that the differences lie more in the regulatory networks that overlie the core mechanisms. For example, the centralspindlin complex with the mitotic kinesin-like protein (MKLP) and its associated Rho/Rac GAP (MgcRacGap) may principally lead to cycling of Rho and possibly inactivation of Rac in order to promote myosin II-based contractility at the cleavage furrow. With respect to myosin II, this regulation occurs through the local activation of Rho kinase, which activates myosin II thick filament assembly and myosin II mechanochemistry through the phosphorylation of the regulatory light chain. Evidence for this pathway comes from the fact that inhibition of the Rho pathway blocks myosin RLC phosphorylation and myosin recruitment. Further, RLC phosphorylation appears to be required for bipolar thick filament assembly as well as full activation of the actin-activated myosin ATPase activity. In *Dictyostelium*, Rho kinase is absent. Since the actin-activated myosin ATPase activity only leads to about three- to fivefold activation (compared to 20- to 30-fold for many other myosin IIs) and the *Dictyostelium* myosin II is not rate limiting for cytokinesis for at least a tenfold range of activity,[35,48] Rho kinase may not be needed. For *Dictyostelium* myosin II, deletion of the RLC binding site (RLCBS) alleviates the inhibition of the actin-activated ATPase activity that comes from the unphosphorylated RLC. This ΔRLCBS myosin II and deletion of both light chain binding site (ΔBLCBS) myosin II still localize to the cleavage furrow cortex in *Dictyostelium*. Recent studies using mammalian cells reveals that a similar ΔRLCBS myosin IIA also localizes to the cleavage furrow and can provide full function in the presence of Rho pathway inhibitors.[163] Similarly, in *Drosophila* cells, phosphomimic mutations at the RLC-activating phosphorylation sites are able to rescue Rho kinase inhibition, further demonstrating that the Rho pathway principally activates the myosin II.[187] There are additional effects of the Rho pathway on formin-mediated actin assembly, however. Finally, mutant myosin IIs where the motor domain has been deleted is also sufficient for cleavage furrow targeting in *Dictyostelium* and mammalian cells.[162,163] Overall, these observations collectively suggest that the regulation of myosin II by these pathways occurred much later than the core cell division mechanism and likely co-evolved with a need to have greater regulatory control over myosin II-based contractility.

One principal role of the anillin proteins, including anillin and the *S. pombe* mid1p, may be to similarly function with myosin II-based contractility through cooperative interactions akin to cortexillin in *Dictyostelium*.[188] Anillin has a number of features that make it attractive for being a cooperator of myosin-based contractility. In *C. elegans anillin*-deficient cells, myosin II still accumulates at the cleavage furrow, though it does so more symmetrically and uniformly than in wild-type *C. elegans* embryos.[84] Further, in wild-type embryos, first cleavage furrow ingression typically occurs asymmetrically (faster from one side than the other). This asymmetry is abolished by *anillin* depletion. Analogously, deletion of *cortexillin I* also led to altered furrow ingression dynamics and a disruption in the symmetry of furrow ingression; in *Dictyostelium*, this is reversed: Wild-type furrows ingress in a highly symmetrical fashion whereas *cortexillin* deletion leads to greater asymmetry.[18,64] Therefore, these observations are consistent with the idea that anillin/cortexillin works cooperatively with myosin II to control the rates and dynamics of furrow ingression.

Mid1p is thought to play a similar organizing role. In *S. pombe*, mid1p is among the first proteins to arrive at the nodes that contribute to early metaphase CR assembly.[176]

However, mid1p is not required for myosin II ring formation if cell cycle progression through metaphase and anaphase is slowed down.[181] Thus, while mid1p certainly helps with speed of actin-myosin II ring assembly, it is not essential, and this result is consistent with the idea that mid1p is an efficiency factor, acting cooperatively with myosin II to facilitate CR assembly.

7.5.15 Conclusion

Our view is that there are universal principles that drive cell division in amoeboid and animal cells. The core principle is that mechanical stress propagates through the viscoelastic cytoskeletal network, which drives furrow ingression. The critical elements then are the variety of actin crosslinking proteins found in distinct regions of the cortex and how these crosslinkers respond to stress, whether it originates from cell-substrate interactions or myosin II mechanochemistry. This spatial heterogeneity of actin crosslinkers, in combination with the manner in which they unbind from the actin polymer, creates the regional mechanical features that promote furrow ingression. These proteins have activities that are also mechanoresponsive, leading to a control system characterized by mechanical-biochemical coupled feedback loops. As discussed above, the apparent differences in cytokinesis contractile mechanisms across species could be due to differential regulation of a core mechanical-biochemical feedback system. Therefore, these differences may have originated from how the various systems evolved to be regulated rather than from the core biophysical mechanism. Nevertheless, one fascinating area of the future includes determining how each of the mechanical properties themselves is regulated.

Furthermore, many cancer genes encode proteins that play significant roles in cytokinesis. It will be exciting to learn how these proteins contribute to the mechanics and regulation of cytokinesis. Finally, in the future it should be possible for the cytokinesis and cell mechanics fields to leverage this understanding to develop new strategies for targeting cytokinesis with small molecule inhibitors.[189] Interestingly, a feature of nearly all cancer types is that the cancer cells have altered cell mechanics.[190] In much the same way that cell mechanics play a central role in cytokinesis, they also play a role in cell motility. Some cancer-causing lesions are likely to affect cell mechanics, which can simultaneously impact cytokinesis fidelity (thereby impacting genomic stability) and cell deformability (thereby contributing to metastasis). Thus, understanding how the regulatory and structural machinery controls these mechanical features of dividing and metastatic cells may allow for very novel strategies for diagnosis and therapeutic intervention that can protect healthy, normal dividing cells while targeting cancer cells.

Acknowledgments

The authors' research is supported by the American Cancer Society (RSG CCG-114122) and the National Institutes of Health (GM066817 and GM086704).

References

[1] Li, R. Cytokinesis in development and disease: Variations on a common theme. *Cell. Mol. Life Sci.* **2007**, *64*, 3044–3058.
[2] Cabernard, C.; Prehoda, K. E.; Doe, C. Q. A spindle-independent cleavage furrow positioning pathway. *Nature* **2010**, *467*, 91–94.
[3] Ou, G.; Stuurman, N.; D'Ambrosio, M.; Vale, R. D. Polarized myosin produces unequal-size daughters during asymmetric cell division. *Science* **2010**, *330*, 677–680.
[4] Larson, S. M.; Lee, H. J.; Hung, P.-h.; Matthews, L. M.; Robinson, D. N.; Evans, J. P. Cortical mechanics and meiosis II completion in mammalian oocytes are mediated by myosin-II and ezrin-radixin-moesin (ERM) proteins. *Mol. Biol. Cell* **2010**, *21*, 3182–3192.
[5] Ravid, K.; Lu, J.; Zimmet, J. M.; Jones, M. R. Roads to polyploidy: The megakaryocyte example. *J. Cell. Physiol.* **2002**, *190*, 7–20.
[6] Margall-Ducos, G.; Celton-Morizur, S.; Couton, D.; Bregerie, O.; Desdouets, C. Liver tetraploidization is controlled by a new process of incomplete cytokinesis. *J. Cell Sci.* **2007**, *120*, 3633–3639.
[7] Wilker, E. W.; van Vugt, M. A.; Artim, S. A.; Huang, P. H.; Petersen, C. P.; Reinhardt, H. C.; Feng, Y.; Sharp, P. A.; Sonenberg, N.; White, F. M.; Yaffe, M. B. 14-3-3sigma controls mitotic translation to facilitate cytokinesis. *Nature* **2007**, *446*, 329–332.
[8] Hermeking, H. The 14-3-3 cancer connection. *Nat. Rev. Cancer* **2003**, *3*, 931–943.
[9] Eggert, U. S.; Mitchison, T. J.; Field, C. M. Animal cytokinesis: From parts list to mechanisms. *Annu. Rev. Biochem.* **2006**, *75*, 543–566.
[10] Glotzer, M. The molecular requirements for cytokinesis. *Science* **2005**, *307*, 1735–1739.
[11] Reichl, E. M.; Effler, J. C.; Robinson, D. N. The stress and strain of cytokinesis. *Trends Cell Biol.* **2005**, *15*, 200–206.
[12] Robinson, D. N.; Cavet, G.; Warrick, H. M.; Spudich, J. A. Quantitation of the distribution and flux of myosin-II during cytokinesis. *BMC Cell Biol.* **2002**, *3*, 4.
[13] Janetopoulos, C.; Borleis, J.; Vazquez, F.; Iijima, M.; Devreotes, P. Temporal and spatial regulation of phosphoinositide signaling mediates cytokinesis. *Dev. Cell* **2005**, *8*, 467–477.
[14] Echard, A. Membrane traffic and polarization of lipid domains during cytokinesis. *Biochem. Soc. Trans.* **2008**, *36*(Pt. 3), 395–399.
[15] Emoto, K.; Inadome, H.; Kanaho, Y.; Narumiya, S.; Umeda, M. Local change in phospholipid composition at the cleavage furrow is essential for completion of cytokinesis. *J. Biol. Chem.* **2005**, *280*, 37901–37907.
[16] Hategan, A.; Law, R.; Kahn, S.; Discher, D. E. Adhesively-tensed cell membranes: Lysis kinetics and atomic force microscopy probing. *Biophys. J.* **2003**, *85*, 2746–2759.
[17] Gauthier, N. C.; Rossier, O. M.; Mathur, A.; Hone, J. C.; Sheetz, M. P. Plasma membrane area increases with spread area by exocytosis of a GPI-anchored protein compartment. *Mol. Biol. Cell* **2009**, *20*, 3261–3272.
[18] Girard, K. D.; Chaney, C.; Delannoy, M.; Kuo, S. C.; Robinson, D. N. Dynacortin contributes to cortical viscoelasticity and helps define the shape changes of cytokinesis. *EMBO J.* **2004**, *23*, 1536–1546.
[19] Girard, K. D.; Kuo, S. C.; Robinson, D. N. Dictyostelium myosin-II mechanochemistry promotes active behavior of the cortex on long time-scales. *Proc. Natl. Acad. Sci. USA* **2006**, *103*, 2103–2108.
[20] Stewart, M. P.; Helenius, J.; Toyoda, Y.; Ramanathan, S. P.; Muller, D. J.; Hyman, A. A. Hydrostatic pressure and the actomyosin cortex drive mitotic cell rounding. *Nature* **2011**, *469*, 226–230.
[21] Mabuchi, I.; Okuno, M. The effect of myosin antibody on the division of starfish blastomeres. *J. Cell Biol.* **1977**, *74*, 251–263.
[22] De Lozanne, A.; Spudich, J. A. Disruption of the Dictyostelium myosin heavy chain gene by homologous recombination. *Science* **1987**, *236*, 1086–1091.
[23] Schroeder, T. E. Actin in dividing cells: Contractile ring filaments bind heavy meromyosin. *Proc. Natl. Acad. Sci. USA* **1973**, *70*, 1688–1692.
[24] Knecht, D. A.; Loomis, W. F.; Antisense, R. N. A. inactivation of myosin heavy chain gene expression in Dictyostelium discoideum. *Science* **1987**, *236*, 1081–1086.
[25] Bezanilla, M.; Forsburg, S. L.; Pollard, T. D. Identification of a second myosin-II in Schizosaccharomyces pombe: Myp2p is conditionally required for cytokinesis. *Mol. Biol. Cell* **1997**, *8*, 2693–2705.
[26] Rappaport, R. *Cytokinesis in Animal Cells*; Cambridge University Press: Cambridge, 1996.
[27] Sellers, J. R. Myosins A diverse superfamily. *Biochim. Biophys. Acta* **2000**, *1496*, 3–22.

[28] Murphy, C. T.; Rock, R. S.; Spudich, J. A. A myosin II mutation uncouples ATPase activity from motility and shortens step size. *Nat. Cell Biol.* **2001**, *3*, 311–315.

[29] Spudich, J. A. The myosin swinging cross-bridge model. *Nat. Rev. Mol. Cell Biol.* **2001**, *2*, 387–392.

[30] Laakso, J. M.; Lewis, J. H.; Shuman, H.; Ostap, E. M. Myosin I can act as a molecular force sensor. *Science* **2008**, *321*, 133–136.

[31] Kovacs, M.; Thirumurugan, K.; Knight, P. J.; Sellers, J. R. Load-dependent mechanism of nonmuscle myosin 2. *Proc. Natl. Acad. Sci. USA* **2007**, *104*, 9994–9999.

[32] Altman, D.; Sweeney, H. L.; Spudich, J. A. The mechanism of myosin VI translocation and its load-induced anchoring. *Cell* **2004**, *116*, 737–749.

[33] Gebhardt, J. C.; Clemen, A. E.; Jaud, J.; Rief, M. Myosin-V is a mechanical ratchet. *Proc. Natl. Acad. Sci. USA* **2006**, *103*, 8680–8685.

[34] Purcell, T. J.; Sweeney, H. L.; Spudich, J. A. A force-dependent state controls the coordination of processive myosin V. *Proc. Natl. Acad. Sci. USA* **2005**, *102*(39), 13873–13878.

[35] Ostrow, B. D.; Chen, P.; Chisholm, R. L. Expression of a myosin regulatory light chain phosphorylation site mutant complements the cytokinesis and developmental defects of Dictyostelium RMLC null cells. *J. Cell Biol.* **1994**, *127*, 1945–1955.

[36] Pollard, T. D. Structure and polymerization of Acanthamoeba myosin-II filaments. *J. Cell Biol.* **1982**, *95*, 816–825.

[37] Pepe, F. A.; Drucker, B. The myosin filament VI. Myosin content. *J. Mol. Biol.* **1979**, *130*, 379–393.

[38] Howard, J. Molecular motors: Structural adaptations to cellular functions. *Nature* **1997**, *389*, 561–567.

[39] Niederman, R.; Pollard, T. D. Human platelet myosin. II. In vitro assembly and structure of myosin filaments. *J. Cell Biol.* **1975**, *67*, 72–92.

[40] Verkhovsky, A. B.; Borisy, G. G. Non-sarcomeric mode of myosin II organization in the fibroblast lamellum. *J. Cell Biol.* **1993**, *123*, 637–652.

[41] Egelhoff, T. T.; Lee, R. J.; Spudich, J. A. Dictyostelium myosin heavy chain phosphorylation sites regulate myosin filament assembly and localization in vivo. *Cell* **1993**, *75*, 363–371.

[42] Breckenridge, M. T.; Dulyaninova, N. G.; Egelhoff, T. T. Multiple regulatory steps control mammalian nonmuscle myosin II assembly in live cells. *Mol. Biol. Cell* **2009**, *20*, 338–347.

[43] Liang, W.; Warrick, H. M.; Spudich, J. A. A structural model for phosphorylation control of Dictyostelium myosin II thick filament assembly. *J. Cell Biol.* **1999**, *147*, 1023–1038.

[44] Hostetter, D.; Rice, S.; Dean, S.; Altman, D.; McMahon, P. M.; Sutton, S.; Tripathy, A.; Spudich, J. A. Dictyostelium myosin bipolar thick filament formation: Importance of charge and specific domains of the myosin rod. *PLoS Biol.* **2004**, *2*, e356.

[45] Clarke, M.; Spudich, J. A. Biochemical and structural studies of actomyosin-like proteins from non-muscle cells. *J. Mol. Biol.* **1974**, *86*, 209–222.

[46] Clarke, M.; Spudich, J. A. Nonmuscle contractile proteins: The role of actin and myosin in cell motility and shape determination. *Annu. Rev. Biochem.* **1977**, *46*, 797–822.

[47] Haugwitz, M.; Noegel, A. A.; Karakesisoglou, J.; Schleicher, M. Dictyostelium amoebae that lack G-actin-sequestering profilins show defects in F-actin content, cytokinesis, and development. *Cell* **1994**, *79*, 303–314.

[48] Reichl, E. M.; Ren, Y.; Morphew, M. K.; Delannoy, M.; Effler, J. C.; Girard, K. D.; Divi, S.; Iglesias, P. A.; Kuo, S. C.; Robinson, D. N. Interactions between myosin and actin crosslinkers control cytokinesis contractility dynamics and mechanics. *Curr. Biol.* **2008**, *18*, 471–480.

[49] Podolski, J. L.; Steck, T. L. Length distribution of F-actin in *Dictyostelium discoideum*. *J. Biol. Chem.* **1990**, *265*, 1312–1318.

[50] Biron, D.; Moses, E. The effect of α-actinin on the length distribution of F-actin. *Biophys. J.* **2004**, *86*, 3284–3290.

[51] Kamasaki, T.; Osumi, M.; Mabuchi, I. Three-dimensional arrangement of F-actin in the contractile ring of fission yeast. *J. Cell Biol.* **2007**, *178*, 765–771.

[52] Field, C. M.; Alberts, B. M. Anillin, a contractile ring protein that cycles from the nucleus to the cell cortex. *J. Cell Biol.* **1995**, *131*, 165–178.

[53] Straight, A. F.; Field, C. M.; Mitchison, T. J. Anillin binds nonmuscle myosin II and regulates the contractile ring. *Mol. Biol. Cell* **2005**, *16*, 193–201.

[54] Piekny, A. J.; Maddox, A. S. The myriad roles of anillin during cytokinesis. *Semin. Cell Dev. Biol.* **2010**, *21*, 881–891.

[55] Paoletti, A.; Chang, F. Analysis of mid1p, a protein required for placement of the cell division site, reveals a link between the nucleus and the cell surface in fission yeast. *Mol. Biol. Cell* **2000**, *11*, 2757–2773.

[56] Berlin, A.; Paoletti, A.; Chang, F. Mid2p stabilizes septin rings during cytokinesis in fission yeast. *J. Cell Biol.* **2003**, *160*, 1083–1092.

[57] Tasto, J. J.; Morrell, J. L.; Gould, K. L. An anillin homologue, Mid2p, acts during fission yeast cytokinesis to organize the septin ring and promote cell separation. *J. Cell Biol.* **2003**, *160*, 1093–1103.

[58] Faix, J.; Steinmetz, M.; Boves, H.; Kammerer, R. A.; Lottspeich, F.; Mintert, U.; Murphy, J.; Stock, A.; Aebi, U.; Gerisch, G. Cortexillins, major determinants of cell shape and size, are actin-bundling proteins with a parallel coiled-coil tail. *Cell* **1996**, *86*, 631–642.

[59] Faix, J.; Clougherty, C.; Konzok, A.; Mintert, U.; Murphy, J.; Albrecht, R.; Mühlbauer, B.; Kuhlmann, J. The IQGAP-related protein DGAP1 interacts with Rac and is involved in the modulation of the F-actin cytoskeleton and control of cell motility. *J. Cell Sci.* **1998**, *111*, 3059–3071.

[60] Faix, J.; Dittrich, W. DGAP1, a homologue of rasGTPase activating proteins that controls growth, cytokinesis, and development in *Dictyostelium discoideum*. *FEBS Lett.* **1996**, *394*, 251–257.

[61] Faix, J.; Weber, I.; Mintert, U.; Köhler, J.; Lottspeich, F.; Marriott, G. Recruitment of cortexillin into the cleavage furrow is controlled by Rac1 and IQGAP-related proteins. *EMBO J.* **2001**, *20*, 3705–3715.

[62] Octtaviani, E.; Effler, J. C.; Robinson, D. N. Enlazin, a natural fusion of two classes of canonical cytoskeletal proteins, contributes to cytokinesis dynamics. *Mol. Biol. Cell* **2006**, *17*, 5275–5286.

[63] Weber, I.; Gerisch, G.; Heizer, C.; Murphy, J.; Badelt, K.; Stock, A.; Schwartz, J.-M.; Faix, J. Cytokinesis mediated through the recruitment of cortexillins into the cleavage furrow. *EMBO J.* **1999**, *18*, 586–594.

[64] Weber, I.; Neujahr, R.; Du, A.; Köhler, J.; Faix, J.; Gerisch, G. Two-step positioning of a cleavage furrow by cortexillin and myosin II. *Curr. Biol.* **2000**, *10*, 501–506.

[65] Ren, Y.; Effler, J. C.; Norstrom, M.; Luo, T.; Firtel, R. A.; Iglesias, P. A.; Rock, R. S.; Robinson, D. N. Mechanosensing through cooperative interactions between myosin II and the actin crosslinker cortexillin I. *Curr. Biol.* **2009**, *19*, 1421–1428.

[66] Robinson, D. N.; Spudich, J. A. Dynacortin, a genetic link between equatorial contractility and global shape control discovered by library complementation of a Dictyostelium discoideum cytokinesis mutant. *J. Cell Biol.* **2000**, *150*, 823–838.

[67] Robinson, D. N.; Ocon, S. S.; Rock, R. S.; Spudich, J. A. Dynacortin is a novel actin bundling protein that localizes to dynamic actin structures. *J. Biol. Chem.* **2002**, *277*, 9088–9095.

[68] Prassler, J.; Stocker, S.; Marriott, G.; Heidecker, M.; Kellermann, J.; Gerisch, G. Interaction of a Dictyostelium member of the plastin/fimbrin family with actin filaments and actin-myosin complexes. *Mol. Biol. Cell* **1997**, *8*, 83–95.

[69] Larochelle, D. A.; Vithalani, K. K.; DeLozanne, A. A novel member of the rho family of small GTP-binding proteins is specifically required for cytokinesis. *J. Cell Biol.* **1996**, *133*, 1321–1329.

[70] Larochelle, D. A.; Vithalani, K. K.; DeLozanne, A. Role of Dictyostelium racE in cytokinesis: Mutational analysis and localization studies by the use of green fluorescent protein. *Mol. Biol. Cell* **1997**, *8*, 935–944.

[71] Zhang, W.; Robinson, D. N. Balance of actively generated contractile and resistive forces controls cytokinesis dynamics. *Proc. Natl. Acad. Sci. USA* **2005**, *102*, 7186–7191.

[72] Gerald, N.; Dai, J.; Ting-Beall, H. P.; DeLozanne, A. A role for Dictyostelium RacE in cortical tension and cleavage furrow progression. *J. Cell Biol.* **1998**, *141*, 483–492.

[73] Robinson, D. N. 14-3-3, an integrator of cell mechanics and cytokinesis. *Small GTPases* **2010**, *1*, 1–5.

[74] Zhou, Q. Q.; Kee, Y.-S.; Poirier, C. C.; Jelinek, C.; Osborne, J.; Divi, S.; Surcel, A.; Tran, M. E.; Eggert, U. S.; Müller-Taubenberger, A.; Iglesias, P. A.; Cotter, R. C.; Robinson, D. N. 14-3-3 coordinates microtubules, Rac and myosin II to control cell mechanics and cytokinesis. *Curr. Biol.* **2010**, *20*, 1881–1889.

[75] Mukhina, S.; Wang, Y. L.; Murata-Hori, M. alpha-Actinin is required for tightly regulated remodeling of the actin cortical network during cytokinesis. *Dev. Cell* **2007**, *13*, 554–565.

[76] Reichl, E. M.; Robinson, D. N. Putting the brakes on cytokinesis with alpha-actinin. *Dev. Cell* **2007**, *13*, 460–462.

[77] Kasza, K.; Nakamura, F.; Hu, S.; Kollmannsberger, P.; Bonakdar, N.; Fabry, B.; Stossel, T.; Wang, N.; Weitz, D. Filamin A is essential for active cell stiffening but not passive stiffening under external force. *Biophys. J.* **2009**, *96*, 4326–4335.

[78] Cukier, I. H.; Li, Y.; Lee, J. M. Cyclin B1/Cdk1 binds and phosphorylates Filamin A and regulates its ability to cross-link actin. *FEBS Lett.* **2007**, *581*, 1661–1672.

[79] Khaire, N.; Muller, R.; Blau-Wasser, R.; Eichinger, L.; Schleicher, M.; Rief, M.; Holak, T. A.; Noegel, A. A. Filamin-regulated F-actin assembly is essential for morphogenesis and controls phototaxis in Dictyostelium. *J. Biol. Chem.* **2007**, *282*, 1948–1955.

[80] Tseng, Y.; Esue, K. M.; Wirtz, O. D. The bimodal role of filamin in controlling the architecture and mechanics of F-actin networks. *J. Biol. Chem.* **2004**, *279*, 1819–1826.

[81] Gardel, M. L.; Nakamura, F.; Hartwig, J. H.; Crocker, J. C.; Stossel, T. P.; Weitz, D. Prestressed F-actin networks cross-linked by hinged filamins replicate mechanical properties of cells. *Proc. Natl. Acad. Sci. USA* **2006**, *103*, 1762–1767.

[82] Field, C. M.; Kellogg, D. Septins: Cytoskeletal polymers or signalling GTPases? *Trends Cell Biol.* **1999**, *9*, 387–394.

[83] Robinson, D. N.; Cooley, L. Stable intercellular bridges in development: The cytoskeleton lining the tunnel. *Trends Cell Biol.* **1996**, *6*, 474–479.

[84] Maddox, A. S.; Lewellyn, L.; Desai, A.; Oegema, K. Anillin and the septins promote asymmetric ingression of the cytokinetic furrow. *Dev. Cell* **2007**, *12*, 827–835.

[85] Maupin, P.; Pollard, T. D. Arrangement of actin filaments and myosin-like filaments in the contractile ring and of actin-like filaments in the mitotic spindle of dividing HeLa cells. *J. Ultrastruct. Res.* **1986**, *94*, 92–103.

[86] Evangelista, M.; Blundell, K.; Longtine, M. S.; Chow, C. J.; Adames, N.; Pringle, J. R.; Peter, M.; Boone, C. Bni1p, a yeast formin linking cdc42p and the actin cytoskeleton during polarized morphogenesis. *Science* **1997**, *276*, 118–122.

[87] Severson, A. F.; Baille, D. L.; Bowerman, B. A formin homology protein and a profilin are required for cytokinesis and Arp2/3-independent assembly of cortical microfilaments in C. elegans. *Curr. Biol.* **2002**, *12*, 2066–2075.

[88] Kovar, D. R.; Pollard, T. D. Insertional assembly of actin filament barbed ends in association with formins produces piconewton forces. *Proc. Natl. Acad. Sci. USA* **2004**, *101*, 14725–14730.

[89] Pruyne, D.; Evangelista, M.; Yang, C.; Bi, E.; Zigmond, S.; Bretscher, A.; Boone, C. Role of formins in actin assembly: Nucleation and barbed-end association. *Science* **2002**, *297*, 612–615.

[90] Fishkind, D. J.; Wang, Y.-L. Orientation and three-dimensional organization of actin filaments in dividing cultured cells. *J. Cell Biol.* **1993**, *123*, 837–848.

[91] Isambert, H.; Venier, P.; Maggs, A. C.; Fattoum, A.; Kassab, R.; Pantaloni, D.; Carlier, M. F. Flexibility of actin filaments derived from thermal fluctuations. Effect of bound nucleotide, phalloidin, and muscle regulatory proteins. *J. Biol. Chem.* **1995**, *270*, 11437–11444.

[92] MacKintosh, F. C.; Kas, J.; Janmey, P. A. Elasticity of semiflexible biopolymer networks. *Phys. Rev. Lett.* **1995**, *75*, 4425–4428.

[93] Xu, J.; Tseng, Y.; Wirtz, D. Strain hardening of actin filament networks. Regulation by the dynamic cross-linking protein alpha-actinin. *J. Biol. Chem.* **2000**, *275*, 35886–35892.

[94] Xu, J.; Wirtz, D.; Pollard, T. D. Dynamic cross-linking by α-actinin determines the mechanical properties of actin filament networks. *J. Biol. Chem.* **1998**, *273*, 9570–9576.

[95] Tseng, Y.; Wirtz, D. Mechanics and multiple-particle tracking microheterogeneity of alpha-actinin-cross-linked actin filament networks. *Biophys. J.* **2001**, *81*, 1643–1656.

[96] Crocker, J. C.; Hoffman, B. D. Multiple-particle tracking and two-point microrheology in cells. *Meth. Cell Biol.* **2007**, *83*, 141–178.

[97] Choquet, D.; Felsenfeld, D. P.; Sheetz, M. P. Extracellular matrix rigidity causes strengthening of integrin-cytoskeleton linkages. *Cell* **1997**, *88*, 39–48.

[98] Feneberg, W.; Westphal, M.; Sackmann, E. Dictyostelium cells′ cytoplasm as an active viscoplastic body. *Eur. Biophys. J.* **2001**, *30*, 284–294.

[99] Bausch, A. R.; Hellerer, U.; Essler, M.; Aepfelbacher, M.; Sackmann, E. Rapid stiffening of integrin receptor-actin linkages in endothelial cells stimulated with thrombin: A magnetic bead rheology study. *Biophys. J.* **2001**, *80*, 2649–2657.

[100] Bausch, A. R.; Moller, W.; Sackmann, E. Measurement of local viscoelasticity and forces in living cells by magnetic tweezers. *Biophys. J.* **1999**, *76*, 573–579.

[101] Bausch, A. R.; Ziemann, F.; Boulbitch, A. A.; Jacobson, K.; Sackmann, E. Local measurements of viscoelastic parameters of adherent cell surfaces by magnetic bead microrheometry. *Biophys. J.* **1998**, *75*, 2038–2049.

[102] Kuo, S. C. Using optics to measure biological forces and mechanics. *Traffic* **2001**, *2*, 757–763.

[103] Mason, T. G.; Ganesan, K.; van Zanten, J. H.; Wirtz, D.; Kuo, S. C. Particle tracking microrheology of complex fluids. *Phys. Rev. Lett.* **1997**, *79*, 3282–3285.

[104] Yamada, S.; Wirtz, D.; Kuo, S. C. Mechanics of living cells measured by laser tracking microrheology. *Biophys. J.* **2000**, *78*, 1736–1747.

[105] Hiramoto, Y. Mechanical properties of sea urchin eggs. II. Changes in mechanical properties from fertilization to cleavage. *Exp. Cell Res.* **1963**, *32*, 76–88.

[106] Hiramoto, Y. Mechanical properties of the cortex before and during cleavage. *Ann. N. Y. Acad. Sci.* **1990**, *582*, 22–30.

[107] Hochmuth, R. M. Micropipette aspiration of living cells. *J. Biomech.* **2000**, *33*, 15–22.

[108] Yang, L.; Effler, J. C.; Kutscher, B. L.; Sullivan, S. P.; Robinson, D. N.; Iglesias, P. A. Modeling cellular deformations using the level set formalism. *BMC Syst. Biol.* **2008**, *2*, 68.

[109] Evans, E.; Yeung, A. Apparent viscosity and cortical tension of blood granulocytes determined by micropipet aspiration. *Biophys. J.* **1989**, *56*, 151–160.

[110] Matzke, R.; Jacobson, K.; Radmacher, M. Direct, high-resolution measurement of furrow stiffening during division of adherent cells. *Nat. Cell Biol.* **2001**, *3*, 607–610.

[111] Kunda, P.; Pelling, A. E.; Liu, T.; Baum, B. Moesin controls cortical rigidity, cell rounding, and spindle morphogenesis during mitosis. *Curr. Biol.* **2008**, *18*, 91–101.

[112] Robinson, D. N. Cell division: Biochemically controlled mechanics. *Curr. Biol.* **2001**, *11*, R737–R740.

[113] Shigley, J. E.; Mishke, C. R. *Mechanical Engineering Design*; McGraw-Hill College: New York, 1989.

[114] Insall, R.; Mueller-Tautenberger, A.; Machesky, L.; Koehler, J.; Simmeth, E.; Atkinson, S. J.; Weber, I.; Gerisch, G. Dynamics of the Dictyostelium Arp2/3 complex in endocytosis, cytokinesis, and chemotaxis. *Cell Motil. Cytoskel.* **2001**, *50*, 115–128.

[115] Cao, L.-g.; Wang, Y. -l. Mechanisms of the formation of contractile ring in dividing cultured animal cells. I. Recruitment of preexisting actin filaments into the cleavage furrow. *J. Cell Biol.* **1990**, *110*, 1089–1095.

[116] Yoneda, M.; Dan, K. Tension at the surface of the dividing sea-urchin egg. *J. Exp. Biol.* **1972**, *57*, 575–587.

[117] Carlsson, A. E. Contractile stress generation by actomyosin gels. *Phys. Rev. E* **2006**, *74*, 051912-1-6.

[118] Zumdieck, A.; Kruse, K.; Bringmann, H.; Hyman, A. A.; Julicher, F. Stress generation and filament turnover during actin ring constriction. *PLoS ONE* **2007**, *2*, e696.

[119] Effler, J. C.; Kee, Y.-S.; Berk, J. M.; Tran, M. N.; Iglesias, P. A.; Robinson, D. N. Mitosis-specific mechanosensing and contractile protein redistribution control cell shape. *Curr. Biol.* **2006**, *16*, 1962–1967.

[120] Rappaport, R. Cell division: Direct measurement of maximum tension exerted by furrow of echinoderm eggs. *Science* **1967**, *156*, 1241–1243.

[121] Humphrey, D.; Duggan, C.; Saha, D.; Smith, D.; Kas, J. Active fluidization of polymer networks through molecular motors. *Nature* **2002**, *416*, 413–416.

[122] Mizuno, D.; Tardin, C.; Schmidt, C. F.; MacKintosh, F. C. Nonequilibrium mechanics of active cytoskeletal networks. *Science* **2007**, *315*, 370–373.

[123] Koenderink, G. H.; Dogic, Z.; Nakamura, F.; Bendix, P. M.; MacKintosh, F. C.; Hartwig, J. H.; Stossel, T.; Weitz, D. An active biopolymer network controlled by molecular motors. *Proc. Natl. Acad. Sci. USA* **2009**, *106*, 15192–15197.

[124] Hale, C. M.; Sun, S. X.; Wirtz, D. Resolving the role of actomyosin contractility in cell microrheology. *PLoS ONE* **2009**, *4*, e7054.

[125] Bendix, P. M.; Koenderink, G. H.; Cuvelier, D.; Dogic, Z.; Koeleman, B. N.; Brieher, W. M.; Field, C. M.; Mahadevan, L.; Weitz, D. A quantitative analysis of contractility in active cytoskeletal protein networks. *Biophys. J.* **2008**, *94*, 3126–3136.

[126] Pasternak, C.; Spudich, J. A.; Elson, E. L. Capping of surface receptors and concomitant cortical tension are generated by conventional myosin. *Nature* **1989**, *341*, 549–551.

[127] Marion, S.; Guillen, N.; Bacri, J.-C.; Wilhelm, C. Acto-myosin cytoskeleton dependent viscosity and shear-thinning behavior of the amoeba cytoplasm. *Eur. Biophys. J.* **2005**, *34*, 262–272.

[128] Hoffman, B. D.; Massiera, G.; Van Citters, K. M.; Crocker, J. C. The consensus mechanics of cultured mammalian cells. *Proc. Natl. Acad. Sci. USA* **2006**, *103*, 10259–10264.

[129] Merkel, R.; Simson, R.; Simson, D. A.; Hohenadl, M.; Boulbitch, A.; Wallraff, E.; Sackmann, E. A micromechanic study of cell polarity and plasma

membrane cell body coupling in Dictyostelium. *Biophys. J.* **2000**, *79*, 707–719.
[130] Wachsstock, D. H.; Schwarz, W. H.; Pollard, T. D. Affinity of α-actinin determines the structure and mechanical properties of actin filament gels. *Biophys. J.* **1993**, *65*, 205–214.
[131] Wachsstock, D. H.; Schwarz, W. H.; Pollard, T. D. Cross-linker dynamics determine the mechanical properties of actin gels. *Biophys. J.* **1994**, *66*, 801–809.
[132] Zang, J.-H.; Cavet, G.; Sabry, J. H.; Wagner, P.; Moores, S. L.; Spudich, J. A. On the role of myosin-II in cytokinesis: Division of Dictyostelium cells under adhesive and nonadhesive conditions. *Mol. Biol. Cell* **1997**, *8*, 2617–2629.
[133] Entov, V. M.; Hinch, E. J. Effect of a spectrum of relaxation times on the capillary thinning of a filament of elastic liquid. *J. Non-Newtonian Fluid Mech.* **1997**, *72*, 31–53.
[134] Niewöhner, J.; Weber, I.; Maniak, M.; Müller-Taubenberger, A.; Gerisch, G. Talin-null cells of Dictyostelium are strongly defective in adhesion to particle and substrate surfaces and slightly impaired in cytokinesis. *J. Cell Biol.* **1997**, *138*, 349–361.
[135] Nagasaki, A.; Kanada, M.; Uyeda, T. Q. P. Cell adhesion molecules regulate contractile ring-independent cytokinesis in Dictyostelium discoideum. *Cell Res.* **2009**, *19*, 236–246.
[136] Fey, P.; Stephens, S.; Titus, M. A.; Chisholm, R. L. SadA, a novel adhesion receptor in Dictyostelium. *J. Cell Biol.* **2002**, *159*, 1109–1119.
[137] Hibi, M.; Nagasaki, A.; Takahashi, M.; Yamagishi, A.; Uyeda, T. Q. P. Dictyostelium discoideum talin A is crucial for myosin II-independent and adhesion-dependent cytokinesis. *J. Muscle Res. Cell Motil.* **2004**, *25*, 127–140.
[138] Burton, K.; Taylor, D. L. Traction forces of cytokinesis measured with optically modified elastic substrata. *Nature* **1997**, *385*, 450–454.
[139] Kanada, M.; Nagasaki, A.; Uyeda, T. Q. Adhesion-dependent and contractile ring-independent equatorial furrowing during cytokinesis in mammalian cells. *Mol. Biol. Cell* **2005**, *16*, 3865–3872.
[140] Meyers, J.; Craig, J.; Odde, D. J. Potential for control of signaling pathways via cell size and shape. *Curr. Biol.* **2006**, *16*, 1685–1693.
[141] Uyeda, T. Q. P.; Kitayama, C.; Yumura, S. Myosin II-independent cytokinesis in Dictyostelium: Its mechanism and implications. *Cell Struct. Funct.* **2000**, *25*, 1–10.
[142] Effler, J. C.; Iglesias, P. A.; Robinson, D. N. A mechanosensory system controls cell shape during mitosis. *Cell Cycle* **2007**, *6*, 30–35.
[143] Uyeda, T. Q.; Abramson, P. D.; Spudich, J. A. The neck region of the myosin motor domain acts as a lever arm to generate movement. *Proc. Natl. Acad. Sci. USA* **1996**, *93*, 4459–4464.
[144] Yumura, S.; Yoshida, M.; Betapudi, V.; Licate, L. S.; Iwadate, Y.; Nagasaki, A.; Uyeda, T. Q.; Egelhoff, T. T. Multiple myosin II heavy chain kinases: Roles in filament assembly control and proper cytokinesis in Dictyostelium. *Mol. Biol. Cell* **2005**, *16*, 4256–4266.
[145] Mahajan, R. K.; Pardee, J. D. Assembly mechanism of Dictyostelium myosin II: Regulation by K^+, Mg^{2+}, and actin filaments. *Biochemistry* **1996**, *35*, 15504–15514.
[146] Moores, S. L.; Spudich, J. A. Conditional loss-of-myosin-II-function mutants reveal a position in the tail that is critical for filament nucleation. *Mol. Cell* **1998**, *1*, 1043–1050.
[147] Mahajan, R. K.; Vaughan, K. T.; Johns, J. A.; Pardee, J. D. Actin filaments mediate Dictyostelium myosin assembly in vitro. *Proc. Natl. Acad. Sci. USA* **1989**, *86*, 6161–6165.
[148] Tokuraku, K.; Kurogi, R.; Toya, R.; Uyeda, T. Q. P. Novel mode of cooperative binding between myosin and Mg^{2+}-actin filaments in the presence of low concentrations of ATP. *J. Mol. Biol.* **2009**, *386*, 149–162.
[149] Orlova, A.; Egelman, E. H. Cooperative rigor binding of myosin to actin is a function of F-actin structure. *J. Mol. Biol.* **1997**, *265*, 469–474.
[150] Adachi, H.; Takahashi, Y.; Hasebe, T.; Shirouzu, M.; Yokoyama, S.; Sutoh, K. Dictyostelium IQGAP-related protein specifically involved in the completion of cytokinesis. *J. Cell Biol.* **1997**, *137*, 891–898.
[151] Stock, A.; Steinmetz, M. O.; Janmey, P. A.; Aebi, U.; Gerisch, G.; Kammerer, R. A.; Weber, I.; Faix, J. Domain analysis of cortexillin I: Actin-bundling, PIP_2-binding and the rescue of cytokinesis. *EMBO J.* **1999**, *18*, 5274–5284.
[152] Pramanik, M. K.; Iijima, M.; Iwadate, Y.; Yumura, S. PTEN is a mechanosensing signal transducer for myosin II localization in Dictyostelium cells. *Genes to Cells* **2009**, *14*, 821–834.
[153] White, J. G.; Borisy, G. G. On the mechanisms of cytokinesis in animal cells. *J. Theor. Biol.* **1983**, *101*, 289–316.
[154] Canman, J. C.; Lewellyn, L.; Laband, K.; Smerdon, S. J.; Desai, A.; Bowerman, B.; Oegema, K. Inhibition of Rac by the GAP activity of centralspindlin is essential for cytokinesis. *Science* **2008**, *322*, 1543–1546.
[155] Vale, R. D.; Spudich, J. A.; Griffis, E. R. Dynamics of myosin, microtubules, and Kinesin-6 at the cortex during cytokinesis in Drosophila S2 cells. *J. Cell Biol.* **2009**, *186*, 727–738.
[156] Odell, G. M.; Foe, V. E. An agent-based model contrasts opposite effects of dynamic and stable microtubules on cleavage furrow positioning. *J. Cell Biol.* **2008**, *183*, 471–483.
[157] Foe, V. E.; von Dassow, G. Stable and dynamic microtubules coordinately shape the myosin activation zone during cytokinetic furrow formation. *J. Cell Biol.* **2008**, *183*, 457–470.
[158] Hu, C. K.; Coughlin, M.; Field, C. M.; Mitchison, T. J. Cell polarization during monopolar cytokinesis. *J. Cell Biol.* **2008**, *181*, 195–202.
[159] Mishima, M.; Kaitna, S.; Glotzer, M. Central spindle assembly and cytokinesis require a kinesin-like protein/RhoGAP complex with microtubule bundling activity. *Dev. Cell* **2002**, *2*, 41–54.
[160] Chen, Q.; Lakshmikanth, G. S.; Spudich, J. A.; DeLozanne, A. The localization of inner centromeric protein (INCENP) at the cleavage furrow is dependent on Kif12 and involves interactions of the N terminus of INCENP with the actin cytoskeleton. *Mol. Biol. Cell* **2007**, *18*, 3366–3374.
[161] Li, H.; Chen, Q.; Kaller, M.; Nellen, W.; Graf, R.; DeLozanne, A. Dictyostelium Aurora kinase has properties of both Aurora A and Aurora B kinases. *Eukaryotic Cell* **2008**, *7*, 894–905.
[162] Zang, J.-H.; Spudich, J. A. Myosin II localization during cytokinesis occurs by a mechanism that does not require its motor domain. *Proc. Natl. Acad. Sci. USA* **1998**, *95*, 13652–13657.
[163] Beach, J. R.; Egelhoff, T. T. Myosin II recruitment during cytokinesis independent of centralspindlin-mediated phosphorylation. *J. Biol. Chem.* **2009**, *284*, 27377–27383.
[164] Dean, S. O.; Rogers, S. L.; Stuurman, N.; Vale, R. D.; Spudich, J. A. Distinct pathways control recruitment and maintenance of myosin II at the cleavage furrow during cytokinesis. *Proc. Natl. Acad. Sci. USA* **2005**, *102*, 13473–13478.
[165] Novák, B.; Tyson, J. J. Design principles of biochemical oscillators. *Nat. Rev. Mol. Cell Biol.* **2008**, *9*, 981–991.
[166] Carvalho, A.; Desai, A.; Oegema, K. Structural memory in the contractile ring makes the duration of cytokinesis independent of cell size. *Cell* **2009**, *137*, 926–937.
[167] Charras, G. T.; Yarrow, J. C.; Horton, M. A.; Mahadevan, L.; Mitchison, T. J. Non-equilibration of hydrostatic pressure in blebbing cells. *Nature* **2005**, *435*, 365–369.
[168] Mitchison, T. J.; Charras, G. T.; Mahadevan, L. Implications of a poroelastic cytoplasm for the dynamics of animal cell shape. *Semin. Cell Dev. Biol.* **2008**, *19*, 215–223.
[169] Bretschneider, T.; Jonkman, J.; Kohler, J.; Medalia, O.; Barisic, K.; Weber, I.; Steltzer, E. H. K.; Baumeister, W.; Gerisch, G. Dynamic organization of the actin system in the motile cells of *Dictyostelium*. *J. Muscle Res. Cell Motil.* **2002**, *23*, 639–649.
[170] Potma, E. O.; de Boeij, W. P.; Bosgraaf, L.; Roelofs, J.; van Haastert, P. J. M.; Wiersma, D. A. Reduced protein diffusion rate by cytoskeleton in vegetative and polarized Dictyostelium cells. *Biophys. J.* **2001**, *81*, 2010–2019.
[171] Potma, E. O.; de Boeij, W. P.; van Haastert, P. J. M.; Wiersma, D. A. Real-time visualization of intracellular hydrodynamics in single living cells. *Proc. Natl. Acad. Sci. USA* **2001**, *98*, 1577–1582.
[172] Biron, D.; Alvarez-Lacalle, E.; Tlusty, T.; Moses, E. Molecular model of the contractile ring. *Phys. Rev. Lett.* **2005**, *95*, 098102-1-4.
[173] Pelham, R. J.; Chang, F. Actin dynamics in the contractile ring during cytokinesis in fission yeast. *Nature* **2002**, *419*, 82–86.
[174] Takaine, M.; Mabuchi, I. Properties of actin from the fission yeast *Schizosaccharomyces pombe* and interaction with fission yeast profilin. *J. Biol. Chem.* **2007**, *282*, 21683–21694.
[175] Wu, J.-Q.; Pollard, T. D. Counting cytokinesis proteins globally and locally in fission yeast. *Science* **2005**, *310*, 310–314.
[176] Wu, J.-Q.; Kuhn, J. R.; Kovar, D. R.; Pollard, T. D. Spatial and temporal pathway for assembly and constriction of the contractile ring in fission yeast cytokinesis. *Dev. Cell* **2003**, *5*, 723–734.
[177] Wu, J.-Q.; Sirotkin, V.; Kovar, D. R.; Lord, M.; Beltzner, C. C.; Kuhn, J. R.; Pollard, T. D. Assembly of the cytokinetic contractile ring from a broad band of nodes in fission yeast. *J. Cell Biol.* **2006**, *174*, 391–402.

[178] Lord, M.; Sladewski, T. D.; Pollard, T. D.; Yeast, U. C. S. proteins promote actomyosin interactions and limit myosin turnover in cells. *Proc. Natl. Acad. Sci. USA* **2008**, *105*, 8014–8019.
[179] Lord, M.; Pollard, T. D. UCS protein Rng3p activates actin filament gliding by fission yeast myosin-II. *J. Cell Biol.* **2004**, *167*, 315–325.
[180] Vavylonis, D.; Wu, J.-Q.; Hao, S.; O'Shaughnessy, B.; Pollard, T. D. Assembly mechanism of the contractile ring for cytokinesis by fission yeast. *Science* **2008**, *319*, 97–100.
[181] Huang, Y.; Yan, H.; Balasubramanian, M. K. Assembly of normal actomyosin rings in the absence of mid1p and cortical nodes in fission yeast. *J. Cell Biol.* **2008**, *183*, 979–988.
[182] Almonacid, M.; Moseley, J. B.; Janvore, J.; Mayeux, A.; Fraisier, V.; Nurse, P.; Paoletti, A. Spatial control of cytokinesis by cdr2 kinase and mid1/anillin nuclear export. *Curr. Biol.* **2009**, *19*, 961–966.
[183] Clifford, D. M.; Wolfe, B. A.; Roberts-Galbraith, R. H.; McDonald, W. H.; Yates, III J. R.; Gould, K. L. The Clp1/Cdc14 phosphatase contributes to the robustness of cytokinesis by association with anillin-related Mid1. *J. Cell Biol.* **2008**, *181*, 79–88.
[184] Moseley, J. B.; Mayeux, A.; Paoletti, A.; Nurse, P. A spatial gradient coordinates cell size and mitotic entry in fission yeast. *Nature* **2009**, *459*, 857–861.
[185] Coffman, V. C.; Nile, A. H.; Lee, I.-J.; Liu, H.; Wu, J.-Q. Roles of formin nodes and myosin motor activity in Mid1p-dependent contractile-ring assembly during fission yeast cytokinesis. *Mol. Biol. Cell* **2009**, *20*, 5195–5210.
[186] Diez, S.; Gerisch, G.; Anderson, K.; Müller-Taubenberger, A.; Bretschneider, T. Subsecond reorganization of the actin network in cell motility and chemotaxis. *Proc. Natl. Acad. Sci. USA* **2005**, *102*, 7601–7606.
[187] Dean, S. O.; Spudich, J. A. Rho kinase′s role in myosin recruitment to the equatorial cortex of mitotic Drosophila S2 cells is for myosin regulatory light chain phosphorylation. *PLoS ONE* **2006**, *1*, e131.
[188] Piekny, A. J.; Glotzer, M. Anillin is a scaffold protein that links RhoA, actin, and myosin during cytokinesis. *Curr. Biol.* **2008**, *18*, 30–36.
[189] Eggert, U. S.; Kiger, A. A.; Richter, C.; Perlman, Z. E.; Perrimon, N.; Mitchison, T. J.; Field, C. M. Parallel chemical genetic and genome-wide RNAi screens identify cytokinesis inhibitors and targets. *PLoS Biol.* **2004**, *2*, e379.
[190] Suresh, S. Biomechanics and biophysics of cancer cells. *Acta Biomater.* **2007**, *3*, 413–438.